

Review

# Carbon Capture Using Porous Silica Materials

Sumedha M. Amaraweera<sup>1</sup>, Chamila A. Gunathilake<sup>2,5\*</sup>, Oneesha H. P. Gunawardene<sup>2</sup>, Rohan S. Dassanayake<sup>3,\*</sup> and Eun-Bum Cho<sup>4,\*</sup> Yanhai Du<sup>5,\*</sup>

<sup>1</sup> Department of Manufacturing and Industrial Engineering, Faculty of Engineering, University of Peradeniya, Peradeniya 20400, Sri Lanka; sumedha.sma@gmail.com (S.M.A.)

<sup>2</sup> Department of Chemical and Process Engineering, Faculty of Engineering, University of Peradeniya, Peradeniya 20400, Sri Lanka; hishendri1995@gmail.com (O.H.P.G.); chamilag@pdn.ac.lk (C.A.G.)

<sup>3</sup> Department of Biosystems Technology, Faculty of Technology, University of Sri Jayewardenepura, Homagama 10200, Sri Lanka; rdassanayake@sjp.ac.lk (R.S.D.)

<sup>4</sup> Department of Fine Chemistry, Seoul National University of Science and Technology, Seoul 01811, Republic of Korea; echo@seoultech.ac.kr (E.C.)

<sup>5</sup> Department of Applied Engineering & Technology, College of Aeronautics and Engineering, Kent State University, Kent, OH, 44242, USA; ydu5@kent.edu (Y.D.)

\* Correspondence: ydu5@kent.edu (Y.D.), cgunathi@kent.edu (C.A.G.), rdassanayake@sjp.ac.lk (R. S. D.), echo@seoultech.ac.kr (E.C.)

**Abstract:** As the major greenhouse gas, CO<sub>2</sub> gas emission has been noticeably increased over the past decades resulting in global warming and climate change. As a result, it is imperative to reduce the excess CO<sub>2</sub> in the atmosphere to hold “the increase in the global average temperature to well below 2°C (ideally 1.5°C) above pre-industrial levels set by the Paris Agreement on climate change. Among many ways, CO<sub>2</sub> capture technology is considered as the most promising technology among the available technologies. Porous materials such as carbons, silica, zeolites, hollow fibers, and alumina are widely used as CO<sub>2</sub> sorbents. However, among the available porous solid sorbents, porous silica-based materials grabbed a significant attention due to their unique properties including high surface area, pore volume, good thermal and mechanical stability, and low cost. Therefore, development of porous silica materials as a promising CO<sub>2</sub> absorbent is a continuously expanding research area in the current moment. Herein, we aim to visualize a full picture of the porous silica-based materials for CO<sub>2</sub> capture. This review presents a comprehensive study of existing CO<sub>2</sub> capture techniques and highlights the recent progress of different porous silica materials and synthesis processes. CO<sub>2</sub> adsorption capacities of unmodified porous silica materials are less effective as compared with functionalized silica materials. Various research activities have been reported about functionalization of porous silica using amine groups. Therefore, in this review, different synthesis routes of amine-functionalized porous silica materials, CO<sub>2</sub> adsorption capacities, gas selectivity and reusability were discussed. Moreover, the research challenges associated with the porous silica materials and future research directions are summarized.

**Keywords:** CO<sub>2</sub> Capture Technologies; CO<sub>2</sub> Adsorption; Porous Silica; Amine Functionalized Porous Silica; Decarbonization

## 1. Introduction

With exponential growth of industrialization, global warming and climate change have become a global concern and drawn much attention in recent decades [1]. As a solution for these key issues, research activities are developed for capturing carbon dioxide (CO<sub>2</sub>), the major greenhouse gas. However, atmospheric CO<sub>2</sub> measured at NOAA's Mauna Loa Atmospheric Baseline Observatory peaked for 2021 at a monthly average of 419 parts per million (ppm) and it is reported as the highest level since accurate measurements began 63 years ago [2].

The increase of CO<sub>2</sub> concentration results climate change such as rise of global temperature and sea levels, alternative of rainfall patterns, extinction of species, natural disasters such as severe weather events, ranging from flash floods, hurricanes, freezing winters, severe droughts, heat waves, urban smog, and cold streaks [3].

The main types of CO<sub>2</sub> stationary emission sources are power plants, refineries, chemical and petrochemical, iron and steel, gas processing, and cement industries. Due to the growth of industrialization and population, the emission of CO<sub>2</sub> has been drastically increased to approach an irreversible climate change level. To tackle these issues, the international communities led by the United Nation reached a landmark international accord, the Paris Agreement, that was adopted by nearly every nation in 2015 to address climate change and its related issues. Countries around the globe made their “nationally determined contributions” of greenhouse gas reduction and plans to pursue their domestic measures. Different approaches are considered and employed in different countries in order to reduce CO<sub>2</sub> emissions and those are indicated in Table 1.

**Table 1.** Different approaches used in different countries in order to reduce the CO<sub>2</sub> emissions.

Type of approach	Details	References
Improve energy efficiency and promote energy conservation	<ul style="list-style-type: none"> <li>This approach is mainly used in commercial and industrial buildings</li> <li>It shows mainly 10-20% of energy saving</li> <li>It shows extensive capital investment for installation</li> </ul>	[4]
Increase of usage of low carbon or clean fuels such as natural gas, hydrogen or nuclear power; Substitution for Power generation	<ul style="list-style-type: none"> <li>Natural gas emits 40–50% less CO<sub>2</sub> than coal</li> <li>Main advantages of this method are high efficiency and cleaner exhaust gas</li> <li>Main disadvantage is the high cost</li> </ul>	[4]
Deploy renewable energy	<ul style="list-style-type: none"> <li>The renewable energy sources include solar, wind, hydropower, geothermal, oceanic energy and bioenergy</li> <li>This method emits low green house and toxic gases</li> <li>The main limitation is high cost and geographic distribution of the available resources</li> </ul>	[4]
CO <sub>2</sub> capture and storage	<ul style="list-style-type: none"> <li>This method is applicable for large CO<sub>2</sub> point emission sources</li> <li>It can reduce vast amount of CO<sub>2</sub> with capture efficiency of 48%</li> </ul>	[4]

Each of the above-mentioned approaches possesses pros and cons. Among these approaches, the CO<sub>2</sub> capture and storage (CSS) can be used to reduce CO<sub>2</sub> emissions by 85-90% from large emission sources [4]. CCS includes different CO<sub>2</sub> capture, separation, transport, storage technologies, and chemical conversion which are discussed in detail below.

## 2. CO<sub>2</sub> Capture

### 2.1. CO<sub>2</sub> capture technologies

Capture and sequestration of CO<sub>2</sub> (CCS) from aforementioned stationary emission sources has been identified as a paramount option for the issues of global warming and climate change. CCS includes four primary steps known as CO<sub>2</sub> capture, compression, transport, and storage, therefore, developing an efficient and economically feasible technology for the capture and sequestration of CO<sub>2</sub> produced by anthropogenic emissions is critically important. CO<sub>2</sub> capture is the central part of the CCS technology process and gained around 70–80% of the total expensive. However, CSS methods can be classified as for example, (i) Post-combustion (ii) Pre-combustion, and (iii) Oxy-fuel combustion (Oxygen-fired combustion) [5,6].

In *post-combustion capture* technology, it collects and separates the  $\text{CO}_2$  from the emission gases of a combustion system [7–11]. Firstly, flue gas (mainly consists of  $\text{CO}_2$ ,  $\text{H}_2\text{O}$  and  $\text{N}_2$ ) passes through denitrification and desulphurization treatments. As the next step, the flue gas is fed to an absorber which contains solvent. Herein,  $\text{CO}_2$  regeneration occurs. Then the  $\text{CO}_2$ -rich absorbent is sent to a  $\text{CO}_2$ -stripper unit to release the  $\text{CO}_2$  gas. Also,  $\text{CO}_2$ -lean absorbent is sent back to the  $\text{CO}_2$ -absorber unit [1]. Next, the captured  $\text{CO}_2$  is then compressed into supercritical fluid and then transported [1] as shown in Figure 1.

*Pre-combustion capture* is a technology where  $\text{CO}_2$  is captured before the combustion process and  $\text{CO}_2$  is generated as an intermediate co-product of conversion process [12]. The pre-combustion technologies are mainly used in power plants, production of fertilizers and natural gas [13,14].

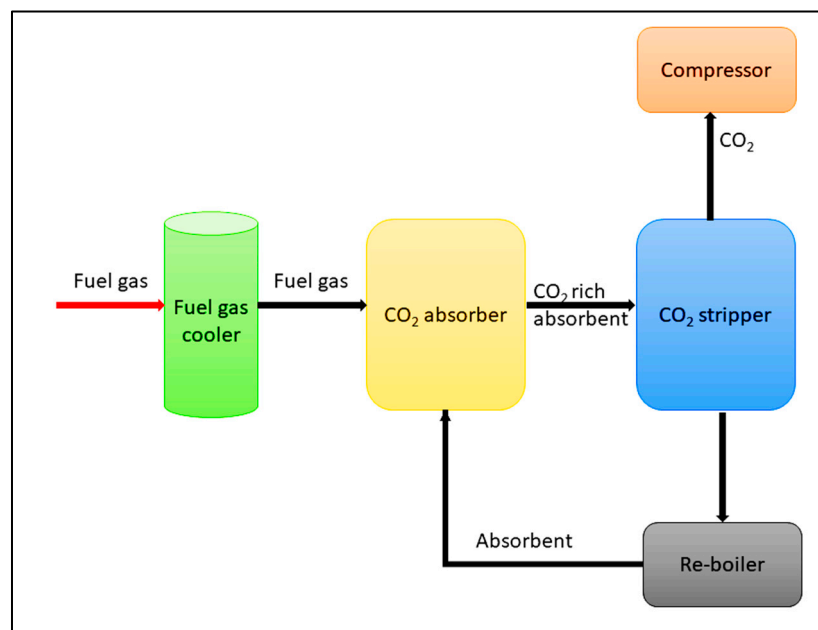


**Figure 1.** Schematic representation of post-combustion technology (Reprinted with permission from Osman et al. [1]).

In *oxyfuel combustion*, the carbon-based fuel consumes in re-circulated flue gas and oxygen ( $\text{O}_2$ ) stream. CSS capture technology is considered expensive due to the high cost of  $\text{O}_2$  separation and production. However, the capture and separation of  $\text{CO}_2$  are reasonably easy compared to other methods and is considered as an energy-saving method [15].

Among the currently available technologies, post-combustion capture has grabbed much attention because it can be easily accomplished, applicable for large scale- power plants, easily managed and required short time for  $\text{CO}_2$  capture compared to other available methods [1]. Post-combustion capture uses different methods for gas separation, and collects  $\text{CO}_2$  by adsorption/desorption, as shown in Table 2, including absorption [6,16], adsorption [6,17] membrane-based technologies [18,19], and cryogenics [20]. Table 2 also depicts the efficiency, advantages and disadvantages of the different types of post-combustion capture technologies.

Absorption process mainly uses liquids to capture  $\text{CO}_2$ . During adsorption, once  $\text{CO}_2$  is separated from the gas, the sorbent should be regenerated by using a stripper, heating, or depressurization. Also, this method is considered as the most established process for  $\text{CO}_2$  separation [21]. In general, adsorbents can be divided into two types, namely, chemical and physical adsorbents (see Table 2 for details).

**Table 2.** Comparison of different post-combustion capture technologies for CO<sub>2</sub> capture.

Technology	Types	Examples	Efficiency (%)	Advantages	Disadvantages	Ref.
<b>Absorption</b>	Chemical	Amines Caustics	> 90	<ul style="list-style-type: none"> <li>• Ability to regenerate</li> <li>• Established method</li> <li>• Very flexible</li> <li>• Reacts rapidly</li> <li>• High absorption capacities</li> </ul>	<ul style="list-style-type: none"> <li>• High energy requirement for regeneration</li> <li>• Environmental problems</li> <li>• High boiling point</li> <li>• Equipment corrosion</li> </ul>	[21,22]
	Physical	Selexol Rectisol fluorinated solvents				
<b>Adsorption</b>	Chemical	Metal Oxides Si based materials	>85	<ul style="list-style-type: none"> <li>• Recyclable</li> <li>• Cost effective</li> <li>• High stability</li> <li>• Adjustable catalytic site and pore sizes</li> <li>• Low energy consumption</li> <li>• Suitable for separating CO<sub>2</sub> from dilute streams</li> </ul>	<ul style="list-style-type: none"> <li>• High energy cost</li> <li>• Limited to process feed rates</li> <li>• Loss of material and pressure drop</li> <li>• Decreased catalytic efficiency</li> <li>• Low adsorption capacities</li> </ul>	[6,21]
	Physical	Carbons Zeolites Si based materials				
<b>Membrane-based technologies</b>	Organic Cellulose Polyphenyleneoxide, derivatives Polydimethylsiloxane Polyamides		>80	<ul style="list-style-type: none"> <li>• Simple device</li> <li>• Easy production process and process flow scheme</li> <li>• Low energy consumption</li> <li>• No phase changes</li> <li>• Capable of maintaining the membrane structure</li> </ul>	<ul style="list-style-type: none"> <li>• Requires a high-cost module and support materials</li> <li>• Not suitable for large volumes of emission gases</li> <li>• Reduced selectivity and separation</li> <li>• Pressure drops across the membrane</li> <li>• Less durability</li> </ul>	[6,21]
	Inorganic	Metallic Ceramics				
<b>Cryogenic distillation</b>				<ul style="list-style-type: none"> <li>• Low capital investment</li> <li>• High reliability</li> <li>• Recovery with high purity of CO<sub>2</sub></li> <li>• Liquid CO<sub>2</sub> production</li> <li>• Not requiring solvents or other components</li> <li>• Easily scalable to industrial-scale applications</li> </ul>	<ul style="list-style-type: none"> <li>• High energy consumption</li> </ul>	[6,21,23]

## 2.2. Criteria for Selecting CO<sub>2</sub> Sorbent Material

Certain economical and technical properties are required in order to select the best solid adsorbent candidate for a particular CO<sub>2</sub> capture application. These criteria are listed and described below.

- Adsorption capacity for CO<sub>2</sub>:

The equilibrium adsorption capacity of a sorbent material is represented by its equilibrium adsorption isotherm. The adsorption capacity is an important parameter when considering the cost. Besides, it causes to reduce the sorbent quantity, and it's the size of the adsorption column. However, to enhance the adsorption capacity of solid sorbents, functionalization has been carried out with existing monoethanolamine (MEA) [24]. The CO<sub>2</sub> working capacity should be in the range of 2-4 mmol/g of the sorbent [25].

- Selectivity for CO<sub>2</sub>:

The adsorption selectivity or selectivity of CO<sub>2</sub> is explained as the sorption uptake ratio of a target gas species compared to another type (as example N<sub>2</sub>) contained in a gaseous mixture under given operation conditions. Therefore, it depends on the purity of the adsorbed gas in the effluent [21]. However, the purity of CO<sub>2</sub> influences transportation and sequestration and, therefore, this criterion plays an important role in CO<sub>2</sub> sequestration [24].

- Adsorption and desorption kinetics:

It is necessary to have fast adsorption/desorption kinetics for CO<sub>2</sub> and it controls the cycle time of a fixed-bed adsorption system. Fast kinetics results in a sharp CO<sub>2</sub> breakthrough curve in which effluent CO<sub>2</sub> concentration changes are measured as a function of time, while slow kinetics provides a distended breakthrough curve. However, both fast and slow adsorption and desorption kinetics impact on the amount of sorbent required. In functionalized solid sorbents, the overall kinetics of CO<sub>2</sub> adsorption mainly depend on the functional groups present, as well as the mass transfer or diffusional resistance of the gas phase through the sorbent structures. The porous support structures of functionalized solid sorbents also can be tailored to minimize the diffusional resistance. The faster an adsorbent can adsorb CO<sub>2</sub> and be desorbed, the less of it will be needed to capture a given volume of flue gas [24].

- Mechanical strength of sorbent particles:

The sorbent must show the stable microstructure and morphological structure in adsorption and regeneration steps. Mainly disintegration of the sorbent particles occurs due to the high volumetric flow rate of flue gas, vibration, and temperature. Apart from that, this could also happen due to abrasion or crushing. Therefore, a sufficient mechanical strength of a sorbent particles is required to keep CO<sub>2</sub> capture process cost-effective [24].

- Chemical stability/tolerance towards impurities:

Solid CO<sub>2</sub> capture sorbents such as amine-functionalized sorbents should be stable in an oxidizing environment of flue gas and should be resistant to common flue gas contaminants [24].

- Regeneration of sorbents:

The regeneration of the sorbent is energy saving and is one of the most important parameters required for improving energy efficiency [26]. Regeneration can be achieved through the adjustment of the thermodynamics of the interaction between CO<sub>2</sub> and the solid adsorbent [24]. Considering regeneration, physisorption is mostly favored as compared with chemisorption since later involves high energy consumption for regeneration.

- Sorbent costs:

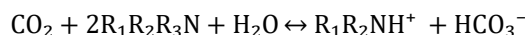
The production cost is the main key point when considering industrial applications at reasonable gas selectivity and adsorption performance [24].

### 2.3. Liquid amine for CO<sub>2</sub> capture

Development of solvents for CO<sub>2</sub> chemical absorption is a major area of research [27]. The ideal solvent should have a high CO<sub>2</sub> absorption capacity and react rapidly and reversibly with CO<sub>2</sub> with minimal heat requirement. The solvent should exhibit the following properties such as stability in oxidative and thermal environment, low vapor pressure, toxicity, flammability, and reasonable production cost [27].

Recently, a most promising CO<sub>2</sub> capture method with chemical absorption is by using liquid amine which can be divided mainly into two groups known as simple alkanolamines and sterically hindered amines [28]. Examples for simple alkanolamines are monoethanolamine (MEA), diethanolamine (DEA) and triethanolamine (TEA) [29,30]. Furthermore, alkanolamines are the most widely used sorbents for CO<sub>2</sub> capture. The structures of alkanolamines include primary, secondary, tertiary amines containing at least one hydroxyl (-OH) group and amine group-(N-R) as shown in Table 3.

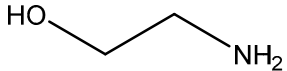
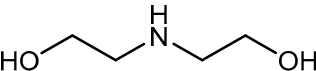
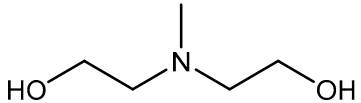
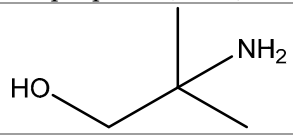
However, these different amine classes have different reaction kinetics with CO<sub>2</sub>, CO<sub>2</sub> absorption capacity and equilibria, stability and corrosion [28]. Advantages and disadvantages among the alkanolamines are shown in Table 3. As shown in equation 1 and 2 below, both primary and secondary amines react with CO<sub>2</sub> to form a carbamate and protonated amine, consuming approximately two moles of amine per mole of CO<sub>2</sub> according to the zwitterion mechanism [31]. According to equation 3, tertiary amines react with CO<sub>2</sub> gas molecules in the presence of H<sub>2</sub>O while forming bicarbonates.



where R<sub>1</sub>, R<sub>2</sub> and R<sub>3</sub> are aryl/alkyl groups

However, García-Abuín et al. [32] observed that MEA produced a mixture of carbamate and bicarbonate as the main reaction products during absorption. The absorption reaction started with the reversible reactions between MEA and CO<sub>2</sub> to form carbamate at low CO<sub>2</sub> loading, followed by the CO<sub>2</sub> hydration to form HCO<sub>3</sub><sup>-</sup>/CO<sub>3</sub><sup>2-</sup> under high CO<sub>2</sub> loading, and accompanied by the hydrolysis of carbamate.

**Table 3.** Comparison between different liquid amines.

Criteria	Alkanolamines			Sterically hindered Amines
	Primary	Secondary	Tertiary	
Examples	Monoethanolamine (MEA)	Diethanolamine (DEA)	N-methyldiethanolamine (MEDA)	2-amino-2-methyl-1-propanol (AMP)
Structure				
CO <sub>2</sub> loading at 59.85 °C (mol CO <sub>2</sub> /mol amine)	0.426 (MEA 30 wt %) [33]	0.404 (DEA 30 wt %) [33]	0.141 (TEA 30 wt %) [33]	0.466 (AMP 30 wt %) [33]
Regeneration efficiency (%) at 90 °C	75.5 [34]	84.89 [34]	95.09 [34]	
Advantages	<ul style="list-style-type: none"> <li>• Inexpensive solvent</li> <li>• Reversible absorption</li> <li>• High selectively (between acid and other gases)</li> <li>• Reacts with CO<sub>2</sub> more rapidly [33]</li> </ul>	<ul style="list-style-type: none"> <li>• Inexpensive solvent</li> <li>• Reversible absorption</li> <li>• High selectively (between acid and other gases)</li> <li>• Reacts with CO<sub>2</sub> more rapidly [33]</li> </ul>	<ul style="list-style-type: none"> <li>• Inexpensive solvent</li> <li>• Reversible absorption</li> <li>• High selectively (between acid and other gases)</li> <li>• High CO<sub>2</sub> absorption capacity energy [34]</li> <li>• Requires low regeneration energy [33]</li> </ul>	<ul style="list-style-type: none"> <li>• High CO<sub>2</sub> absorption capacity</li> <li>• Requires low regeneration energy [34]</li> </ul>
Disadvantages	<ul style="list-style-type: none"> <li>• Lower CO<sub>2</sub> absorption capacity</li> <li>• Requires high regeneration energy</li> <li>• Oxidative degradation occurs in the presence of other gas components</li> <li>• Corrosive</li> <li>• High capital costs [33]</li> </ul>	<ul style="list-style-type: none"> <li>• Lower CO<sub>2</sub> absorption capacity</li> <li>• Requires high regeneration energy</li> <li>• Oxidative degradation occurs in the presence of other gas components</li> <li>• Corrosive</li> <li>• High capital costs [33]</li> </ul>	<ul style="list-style-type: none"> <li>• Reaction rate with CO<sub>2</sub> is low compared to MEA and DEA</li> <li>• Corrosive</li> <li>• High capital costs [33]</li> </ul>	<ul style="list-style-type: none"> <li>• Low reaction rate [34]</li> </ul>



The mechanism of CO<sub>2</sub> capture into MEA solution with different CO<sub>2</sub> loadings is shown in Figure 2.

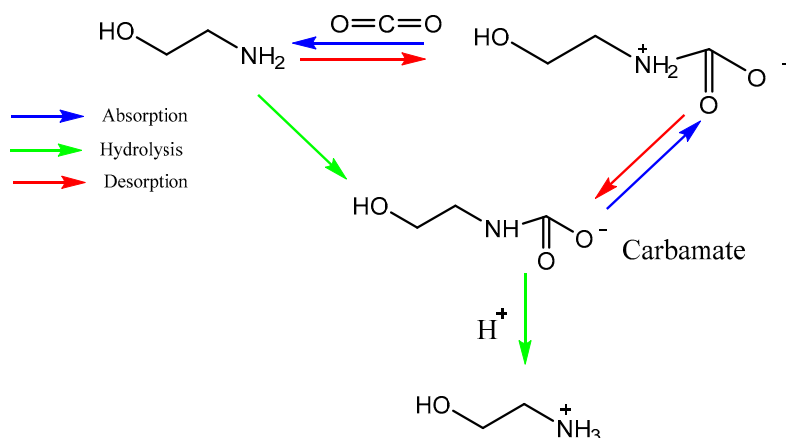


**Figure 2.** Mechanism of CO<sub>2</sub> capture into MEA solution (Reprinted with permission from Lv et al. [31]).

According to Table 3, there are three categories of alkanolamines that show increased capital costs due to requirement of specialized and expensive materials for construction [28]. On the contrary, degradation of alkanolamine causes operational, and environmental problems including high amount of absorbent required, corrosion of equipment, and demanding of energy [24].

MEA is considered as a well-established solvent to separate CO<sub>2</sub> because it can be regenerated easily [35]. On the other hand, Rinprasertmeechai et al. [33] reported the order of CO<sub>2</sub> absorption capacity of the different alkanolamines as MEA > DEA > TEA. Moreover, they have further reported the regeneration ability of the amines in the following order: TEA >> DEA > MEA. According to Table 3, it is clearly shown that, MEA gave the lowest regeneration efficiency of 75.75 % in the first cycle, whereas, TEA offered the highest regeneration performance of 95.09 % [33]. As shown in Table 3, MEA reacts with CO<sub>2</sub> more rapidly compared to MEDA due to the formation of carbamate but MEDA has a higher CO<sub>2</sub> absorption capacity and requires lower energy to regenerate CO<sub>2</sub> [36]. However, Wang et al. [37] found that, when MEA and MEDA are mixed with the appropriate ratio, the energy consumption for CO<sub>2</sub> regeneration is reduced significantly.

Sterically hindered amines are based on primary or secondary amines, with alkyl groups attached to the amino group, which is inhibited from reacting with CO<sub>2</sub> through the effect of steric hindrance [28]. One example of sterically hindered amines is 2-amino-2-methyl-1-propanol (AMP) which reduces the stability of the formed carbamate due to the formation of weak bonds, promoting hydrolysis to form bicarbonate and reducing regeneration energy, but it also releases free amine molecules to react with CO<sub>2</sub>, thus increasing absorption capacity as shown in Table 3. Dave et al. [38] compared the CO<sub>2</sub> absorption of different amine solvents such as MEA, MEDA and NH<sub>3</sub> at various concentrations. They showed that 30wt% AMP-based process has the lowest overall energy requirement over other solvents such as 30% MEA, 30% MEDA, 2.5% NH<sub>3</sub>, and 5% NH<sub>3</sub>.

Recently, ionic liquids (IL) have gained attention due to their properties such as very low vapor pressure, thermal stability, and non-toxicity [39]. The widely used ILs are bis(trifluoromethylsulfonyl)imide (TF<sub>2</sub>N), tetrafluoroborate (BF<sub>4</sub>) and hexafluorophosphate (PF<sub>6</sub>). The main drawbacks of the ILs are high viscosity and they reduce to their blended solutions containing IL and alkanolamines. However, due to the reduction of high viscosity, some rewards are gained such as, increase of energy efficiency, absorption rate, and CO<sub>2</sub> absorption capacity [40,41].



2.4. Comparison between major non-carbonaceous solid sorbents for CO<sub>2</sub> capture and importance of silica materials

Because of disadvantages present in the aqueous amine absorption processes including low contact area between gas and liquid, low CO<sub>2</sub> loading, and absorbent corrosion, as an alternative option, solid adsorption has achieved concern of researchers and industries in recent years [42,43]. A variety of solid adsorbents have been proposed according to their structures and compositions, adsorption mechanisms, and regeneration [43]. Although solid sorbents are inexpensive, they reduce heat capacity, show fast kinetics, increase CO<sub>2</sub> adsorption capacity and selectivity, and exhibit high thermal, chemical, and mechanical stability [43].

However, it is important to improve the CO<sub>2</sub> selectivity and adsorption capacity of a solid sorbent when targeting large volumes of combustion emissions. Recently, most of the commercially available adsorbents are activated carbons, silica, zeolites, hollow fibers, and alumina [6]. These materials show different pore structures, specific surface areas, and surface functional groups, and thus their application fields are highly specific. Table 4 tabulates some typical non-carbonaceous dry adsorbents used for CO<sub>2</sub> capture.

**Table 4.** Advantage and disadvantages of non-carbonaceous adsorbents.

Material types	Examples	Advantages	Disadvantages
Pours silica materials	M41S SBA-n AMS	<ul style="list-style-type: none"><li>• High specific surface area, volume, and good thermal mechanical properties</li></ul>	<ul style="list-style-type: none"><li>• High molecular Porediffusion resistance</li><li>• Decreased adsorption capacity at high temperature [42]</li></ul>
Zeolites	NaY 13X	<ul style="list-style-type: none"><li>• Low production cost</li><li>• Large micropores/mesopores</li><li>• Medium CO<sub>2</sub> adsorption capacity at room temperature</li></ul>	<ul style="list-style-type: none"><li>• Low CO<sub>2</sub> adsorption capacity</li><li>• Moisture-sensitivity</li><li>• High energy consumption [6,43]</li></ul>
Metal organic frameworks (MOFs)	M-MOF- 74 IRMOF-6 USO-2-Ni Zn <sub>4</sub> O(BDC) <sub>3</sub> (MOF-5) USO-1-Al(MIL-53)	<ul style="list-style-type: none"><li>• Large specific surface area</li><li>• Ease of controlling pore sizes</li><li>• High selectivity of CO<sub>2</sub></li></ul>	<ul style="list-style-type: none"><li>• Low CO<sub>2</sub> adsorption capacity at the partial pressure</li><li>• High production cost</li><li>• Complicated synthesis process</li><li>• Moisture-sensitivity</li><li>• Unstable at high temperature [6]</li></ul>
Alkali-based dry adsorbents		<ul style="list-style-type: none"><li>• Possible adsorption and desorption at a low temperature and wet conditions</li></ul>	<ul style="list-style-type: none"><li>• Low adsorption capability (3–11 wt.%)</li><li>• High-temperature reactions</li><li>• Requires high temperatures during desorption</li><li>• Complicated operation [6]</li></ul>
Metal oxides-based adsorbents	CaO, MgO	<ul style="list-style-type: none"><li>• Dry chemical adsorbents</li><li>• Adsorption/desorption at medium to high temperatures</li></ul>	<ul style="list-style-type: none"><li>• High energy consumption</li><li>• High cost for regeneration</li><li>• Complicated process [6]</li></ul>

As mentioned earlier, carbonaceous adsorbents such as activated carbon have been widely used for CO<sub>2</sub> capture due to their wide availability, low cost, and high thermal stability. However, weak CO<sub>2</sub> adsorption of carbonaceous materials in the range of 50–120 °C leads to high sensitivity in temperature and relatively low selectivity in operation [44]. Therefore, much research has focused on non-carbonaceous materials such as mesoporous silica, zeolites, etc. due to their advantages shown in Table 4.

Zeolites are aluminosilicates with a particularly ordered 3-dimensional (3D) microporous structures which have high crystallinity and surface area [44]. The adsorption efficiencies of zeolites are largely affected by their size, charge density, and chemical composition of cations in their porous structures [37]. Literature has reported the change of CO<sub>2</sub> adsorption of zeolites by altering their composition as Si/Al ratio [45] and the exchange with alkali and alkaline-earth cations in the structure of zeolites. However, zeolites present several drawbacks such as relatively low CO<sub>2</sub>/N<sub>2</sub> selectivity and high hydrophilicity [46]. Apart from the above, zeolites show reduced CO<sub>2</sub> adsorption capacity when CO<sub>2</sub>/N<sub>2</sub> mixtures contain moisture and zeolites require high temperatures (> 300 °C) for regeneration [47].

Recently, metal organic frameworks (MOF) have attracted much attention owing to their unique properties such as controllable pore structure and high surface area [48]. However, the MOFs show decreased adsorption capacities when exposed to gas mixtures [46]. Moreover, previous reports indicate that MOFs are promising materials for CO<sub>2</sub> capture in laboratory settings; however, further research is required to confirm their practical applicability [49]. Furthermore, water vapor negatively affects the application of these sorbents. Also, water vapor is adsorbed competitively on physisorbents, and thus decreasing their CO<sub>2</sub> adsorption capacity [50].

Ordered mesoporous silica materials are good candidates because of their high surface area, high pore volume, tunable pore size and good thermal and mechanical stability. So far, mesoporous silica includes the families of MCM (Mobil Company Microporous: M41S, Santa Barbara Amorphous type material (SBA-n), anionic surfactant- template mesoporous silica (AMS) [44]. However, the CO<sub>2</sub> adsorption capacities of them observed at atmospheric pressure are not high. Therefore, many studies based on the synthesis and modification of silica materials containing nano-porous and mesoporous materials for efficient CO<sub>2</sub> capture have been recently reported [51,52].

Several reviews have recently focused on the potential applications of porous silica materials as CO<sub>2</sub> adsorbents. Reddy et al. [53] reported the CO<sub>2</sub> adsorption based on porous materials and in this review, it has mainly reported about MOFs, clay-based adsorbents, porous carbon-based materials and polymer-based adsorbents. However, this recently published review did not mention porous silica materials. Liu et al. [54] also discussed about different porous materials (including porous silica) for post-combustion CO<sub>2</sub> capture but there is limited literature reported about synthesis methods. Therefore, there is a need to identify the best performing porous silica materials and synthesis methods among the thousands of synthesized silica-based materials. Therefore, this review is mainly aimed to discuss the adsorption of CO<sub>2</sub> gas onto different types of porous silica materials and functionalized silica materials. In addition, overview of synthesis processes and comparison between the adsorption capacities are also deeply discussed. Finally, the technical challenges and the future research directions of the porous silica materials for CO<sub>2</sub> adsorption are also presented in this review.

### 3. CO<sub>2</sub> separation methods

There are two general mechanisms involved in the CO<sub>2</sub> capturing using solid sorbents which are known as chemisorption and physisorption. Table 5 represents the comparison between chemisorption and physisorption. However, the difference between the two mechanisms is interactions between the gas molecules and the sorbent surface in adsorption which is shown in Figure 3.

**Table 5.** Comparison between chemisorption and physisorption. .

	Chemisorption	Physisorption
Description	<ul style="list-style-type: none"><li>• Chemical reaction occurs between the solid sorbents and CO<sub>2</sub></li></ul>	<ul style="list-style-type: none"><li>• Depends on the physical properties of CO<sub>2</sub> and the ability to engage in noncovalent interactions with the solid sorbent</li></ul>
Chemical Bonding	<ul style="list-style-type: none"><li>• Covalent Bonding-Occur between functional groups and CO<sub>2</sub> in the surface</li></ul>	<ul style="list-style-type: none"><li>• Week Vander-walls forces-London and Dispersion forces, Occur inside pore walls</li></ul>
Advantages	<ul style="list-style-type: none"><li>• High selectivity</li></ul>	<ul style="list-style-type: none"><li>• Low recycling energy requirements</li><li>• High working capacity</li><li>• High selectivity even in wet environments</li><li>• Fast</li></ul>
Disadvantages	<ul style="list-style-type: none"><li>• High energy required for recycling and the breakage of the chemical bonds</li><li>• Slow reactivity</li></ul>	<ul style="list-style-type: none"><li>• Poor selectivity in binary or mixed gas applications</li></ul>
References	[55,56]	[57–59]

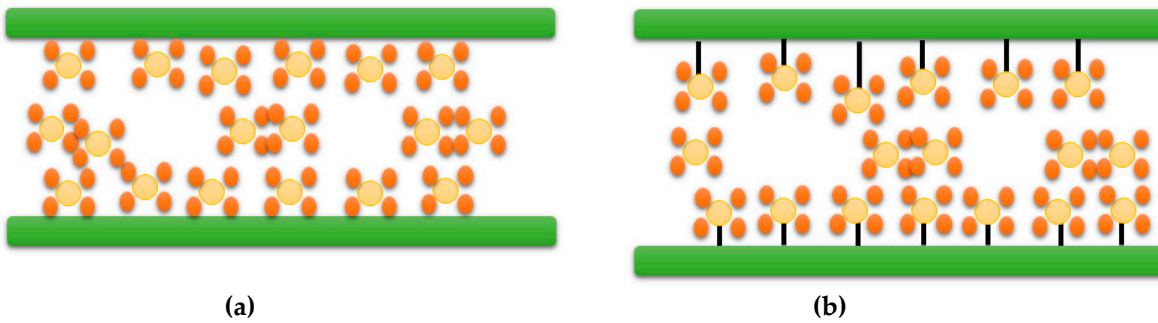


**Figure 3.** Schematic representation of (a) physisorption and (b) chemisorption

The process of CO<sub>2</sub> capturing using solid adsorbent involves in selective separation [24]. The important parameters for solid sorbents are surface tension, pore size, temperature and pressure [24,60]. Adsorption process involves a repeated cycle of adsorption and desorption which is also known as regeneration. The different types of adsorption are shown in Figure 4 such as (i) Pressure Swing Adsorption (PSA) (ii) Temperature Swing Adsorption (TSA) (iii) Electric Swing Adsorption (ESA) and (iv) Vacuum Swing Adsorption (VSA).

Adsorption and desorption occur at low temperature range(40-120 °C) and high temperature range (120-360 °C) in the TSA process, respectively [3]. VSA process involves CO<sub>2</sub> uptake at high pressure and ESA conducts by performing the adsorption–desorption by changing the electrical supply [3]. Activated carbons, MOF, zeolites, activated alumina, and silica gel are mainly used sorbents in TSA and PSA processes while ESA is considered less costly compared to those of both TSA and VSA [60].

Pressure Swing Adsorption (PSA)
<ul style="list-style-type: none"><li>• Adsorption at high pressure, Desorption at low pressure</li><li>• Efficiency &gt;85%</li><li>• Simple to use and requires less energy and investment cost</li></ul>
Temperature Swing Adsorption (TSA)
<ul style="list-style-type: none"><li>• Adsorption at low temperature, Desorption at high temperature</li><li>• Captured CO<sub>2</sub> will be separated by increasing the system temperature using hot air or steam injection</li><li>• Has longer regeneration time</li><li>• 95% purity and 80% recovery is reached</li></ul>
Electric Swing Adsorption (ESA)
<ul style="list-style-type: none"><li>• Adsorption/desorption by varying the electricity supply</li><li>• With a low-voltage current passing through the adsorbent</li></ul>
Vacuum Swing Adsorption (VSA)
<ul style="list-style-type: none"><li>• Frequently used for capturing CO<sub>2</sub></li><li>• Low energy consumption</li><li>• Relative simplicity</li></ul>

Figure 4. The different types of adsorption processes

In contrast, microwave-swing adsorption (MWSA) process has gained much attention in terms of energy management. The main advantage of MWSA is, unlike conventional heating where solids heat through conduction and convection, microwaves are able to provide energy to materials in a direct transfer of the energy to the adsorbent without being absorbed by the adsorbent [62].

4. CO<sub>2</sub> adsorption using mesoporous silica materials (Physisorbents)

4.1. Description about mesoporous silica materials

The mesoporous silica materials are used for a wide variety of applications. Apart from the CO<sub>2</sub> adsorption, those materials are used in various fields such as catalytic and wastewater treatment applications [63]. Mesoporous silica has unique properties such as uniformity of pore distribution (with size between 0.7 and 50 nm), high surface area, (around 1000 m<sup>2</sup>/g) and good thermal stability [64]. The very first synthesized mesoporous silica material is M41S, in the 1990s [65]. However, development of surfactants and synthesis protocols have been able to prepare many types of mesoporous silicas such as MCM-41, SBA-15, SBA-16, FDU-2, MCM-50, KIT-5, etc. with a variety of pore geometries like cubic, and hexagonal, and morphologies like rods, spheres, and discs [66].

In 1990, Mobil Oil Corporation discovered molecular sieves of M41S family consisting of silicate/aluminosilicate [67]. In general, these materials are prepared via the sol-gel method. Three well-defined structural arrangements were identified after studying the effect of surfactant concentration and those are: hexagonal structure (MCM-41), cubic structure (MCM-48), and lamellar structure (MCM-50). Therefore, these materials (M41S family) exhibit mesoporous arrays with amorphous walls of about 10 Å (1 nm) [67]. Moreover, the structural ordering of these M41S family materials can be changed with increasing hydrothermal synthesis temperature and time [67]. These, M41S molecular sieves have attracted great attention in different applications such as catalysis area [68], adsorption [67] and controlled release of drugs [69]. The main advantage of this group is their unique chemical structure consisting with high density of functional silanol groups (Si–OH), pore size, and shape can be modeled during the synthesis process and internal surface can be easily modified with organic and/or inorganic groups [67,70,71].

Santa Barbara Amorphous family (SBA) prepared silica-based materials with well-ordered mesoporous firstly, in 1998 [67]. The material group consists of SBA-2 (hexagonal close-packed array), SBA-12 (three-dimensional hexagonal network), SBA-14 (cubic structure), SBA-15 (two-dimensional hexagonal), and SBA-16 (structured in cubic cage) [67,72]. These nanostructured mesoporous materials are composed of silica-based framework with uniform and well-ordered mesopores, large pores, thick porous walls, high surface area, and high thermal stability [71,73]. Most widely investigated members of the SBA-n family in the literature are SBA-15 and SBA-16. The SBA-15- and SBA-16-based mesoporous arrays are widely utilized as adsorbents [71], catalysts or catalytic [74] and drug deliveries [75].

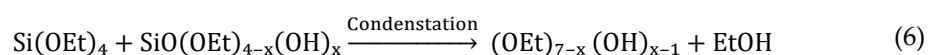
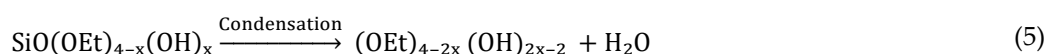
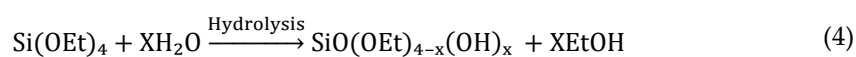
The Fudan University synthesized mesoporous materials family (FDU-n)-based mesoporous silica arrays have well-ordered mesostructures and pore arrangements, high surface area, large and uniform distribution of pore diameter, amorphous pore-wall structures, and thermal and mechanical stability [76]. FDU-1-based mesoporous materials have a 3D face-centered cubic (FCC) structure with large cage-like mesopores while FDU-2 mesoporous array possesses a mesostructured FCC unit cell and well-ordered 3D architecture [71].

On the contrary, the mesoporous material series of the KIT-n family, where  $n = 1, 5$ , or  $6$  are mainly represented by the KIT-1, KIT-5, and KIT-6. However, KIT-1-based mesoporous silicas exhibit a 3D architecture in a disordered framework with high surface area, large pore volume and pore diameter, and thermal and hydrothermal stability [77]. KIT-5-based nanostructured mesoporous materials have a well-ordered 3D cage-like mesopores in a face centered close-packed cubic lattice architecture [71]. In addition, KIT-6 shows a 3D mesoporous amorphous walls with large pore size, uniform pore distribution, high surface area, and thermal stability [71].

Besides, mesoporous silica materials of the M41S, SBA-n, FDU-n, and KIT-n families are used in a wide range of applications such as separation, catalyze, drug release adsorption, sensors, matrix solid phase dispersion (MSPD) and/or solid-phase extraction [71].

#### 4.2. Synthesis procedures

Initially, Stöber et al. [78] discovered an effective method for the synthesis of monodispersed silica particles. This process consists of hydrolysis of tetraethyl orthosilicate (TEOS) using ammonia as a catalyst in water and ethanol solution. This method leads to the synthesis of silica particles [79]. In this reaction, TEOS undergoes a hydrolysis in ethanol/ammonia solution. As a result, it produces silanol monomer (-Si-OH) with the epoxy groups (-Si-OEt) as shown in equation 4. As the next step, as shown equation 5, silanol groups undergoes condensation to produce branched siloxane clusters, which causes to initiate the nucleation and growth of silica particles. Simultaneously, silanol monomers may react with the unhydrolyzed TEOS via the condensation (equation 6) and also participate in the nucleation and growth of silica particles [30]. Moreover, particle size of Stöber silica depends on the concentration of the aqueous ammonia solution and water in ethanol ration [30].



Many experimental factors (such as pH) control the interactions, silica condensation rate, the assembly kinetics and also the nucleation and growth rates [67,80]. The pH is an important factor that influences the charges of silica species. Rates of hydrolysis of silane and condensation of the siloxane bond depend strongly on the charge states. Hydrolysis of the Si-OR bond in silanes could be catalyzed by acid and base conditions but its rate is very slow near the neutral conditions [80].

Sakamoto et al. [81] prepared silica nano particles (NPs) via the evaporation and self-assembly of silicate and quaternarytrialkylmethylammonium as a surfactant. This study shows that size of NPs is dependent on the ratio between the surfactant and silica precursor. Apart from that, Sihler et al.



[82] used dye-stabilized emulsion to synthesize  $\text{SiO}_2$  NPs. Moreover, this synthesis method provides silica capsules and sub particles with exact size control. Monodispersed colloidal silica NPs (diameter of 15-25 nm) were prepared by Murray et al. [83]. In this study, as the silica source, octadecyltrimethoxysilane (OTMS) was used.

In order to increase the pore volume and loading capacity of prepared hollow mesoporous  $\text{SiO}_2$ , researchers have used simple synthesis methods called soft and hard templating methods [84]. Template synthesis of mesoporous materials typically enroll in mainly three steps: template preparation, template directed synthesis of the target materials (sol gel, precipitation, hydrothermal synthesis) and template removal [85].

The hard-templating method involves in nano-casting which uses pre-synthesized mesoporous solids [87]. Hard templating is a facile synthesis method for the fabrication of porous materials with a stable porous structure. The structure replication is very straightforward [85]. This approach utilizes porous “hard templates” (usually mesoporous silica). The pores of these templates are impregnated with a precursor compound for the desired product which is then thermally converted into the product in-situ. The template is finally removed to yield the desired mesoporous material as a negative structural replica of the hard template [85]. However, the method is costly and a time-consuming method. Moreover, the mesoporous parameters such as meso structure and the pore sizes are difficult to change [86].

In contrast, soft templating method, cationic and anionic surfactants or block co-polymers were used as templates [80]. During the synthesis, surfactant or block co-polymers is used as a soft template. Also, the increase of surfactant micelle concentration causes the formation of large assembly or self-assembly of 3D mesoporous [30]. Different 3D micelle structures can be obtained by varying solvent, ratio between the aqueous and non-aqueous and the combination between the co-solvents. Moreover, without any phase separation, silica source interacts with structure directing agent (SDA) because interactions between ions or charged molecules play an important role in the formation of well-defined porous nanostructures [87].

The soft templating method mainly depends on the self-assembly of the surfactant [85]. The process is based on the interactions between inorganics. The mesoporous structure of the final material is obtained after the removal of the pore-templating surfactant or block co-polymers by low-temperature calcination (up to 600 °C) or by different washing techniques (extraction) [85]. Figure 5 represents the synthesis mechanism of mesoporous silica in the presence of a cationic surfactant. The synthesis process of mesoporous silica is carried out using TEOS as the silica source [30]. In this process, surfactant plays a major role such as defining the pore size and pore volume of silica [30]. Cationic surfactant forms micelle structures with water and which leads to arrange the cationic “heads” of the surfactant molecules to the outer side. It resulted in the hydrophobic “tails” collected in the center of each micelle. As the next step, silica molecules cover the micelle surface. Finally, surfactant is removed via calcination or extraction and it resulted in porous silica [30,88,89].

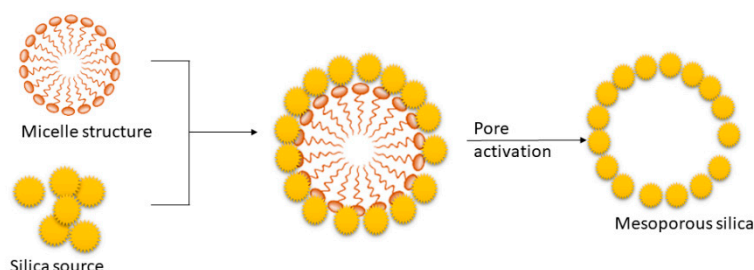


**Figure 5.** Mechanism for the synthesis of mesoporous silica in the presence of a cationic surfactant (Reprinted with permission from Kim et al. [89]).

According to Figure 6, Titania-incorporated organosilica-mesostructures (Ti-MO) were synthesized via condensation method using silica precursors ([3-(trimethoxysilyl) propyl]

isocyanurate and tetraethylorthosilicate) and titanium precursor (titaniumisopropoxide) in the presence of the triblock copolymer, Pluronic P123. The method consists of removing template mainly using two independent steps (i) extraction with a 95% ethanol solution (ii) calcination of sample at 350 °C. This method changes the adsorption and enhanced the structural properties such as specific surface area, micro-porosity, and pore volume.

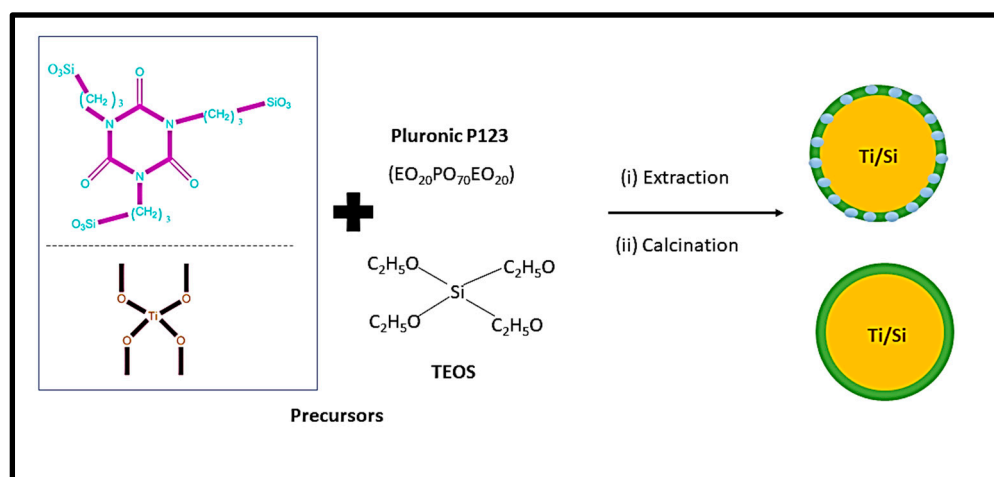


**Figure 6.** Mechanism for the synthesis of mesoporous silica using block copolymer (Re-printed with permission from Gunathilake et al. [90]).

The synthesis of MCM-41 and SBA-15 are preformed using cetrimoniumbromide (CTAB) and Pluronic P123 surfactant. The CTAB is an ionic surfactant and acts as stearidonic acid (SDA) and which causes the formation of a hexagonal array of mesostructured composites [12]. However, as the final step, surfactants are removed by heating in air at high temperatures or by solvent extraction to obtain MCM-41 and SBA-15 [30]. The detailed description about the mechanism was reported by Wu et al. [79] and Hao et al. [90]. Paneka and co-workers have reported the synthesis of MCM-41 from fly ash using a hydrothermal process. However, synthesis of MCM-41 shows reduced BET surface area and increased pore volume, and pore size [91].

Recently, Singh and Polshettiwar [92] reported the synthesis of silica nano-sheets using ammonium hydroxide. They have developed a method to synthesize silica nano-sheets using lamellar micelles as soft templates in a water-cyclohexane solvent mixture. Zhang et al. [19] also reported the large-scale synthesis of mesoporous silica nanoparticles. Reported data shows that various morphologies and particle sizes have been obtained during the synthesis. For synthesis process, the reaction occurred at atmospheric pressure with a sol-gel technique using CTAB as a template.

#### 4.3. Importance of micro-porosity and CO<sub>2</sub> adsorption capacity of the different mesoporous silica materials

The textural properties such as surface area, pore diameter and volume of mesoporous materials are usually determined by the study of nitrogen adsorption-desorption isotherms. The specific surface area is calculated using the volume adsorbed at different relative pressure data by the Brunauer-Emmett-Tellet (BET) method [67]. Apart from that, the pore volume and pore size distribution are usually determined using the Barrett-Joyner-Halenda (BJH) method [67].

However, the textural properties are important parameters when considering CO<sub>2</sub> adsorption using physisorbent materials. However, microporosity of the physisorbents plays a major role in CO<sub>2</sub> gas adsorption because it involves in diffusion of CO<sub>2</sub> gas molecules with sorbent [94]. Table 7 represents the textural properties and CO<sub>2</sub> absorption capacity recorded for different types of ordered mesoporous silica materials studied.

MCM-41 has high porosity and ordered hexagonal pore structure arrangement. However, it showed low CO<sub>2</sub> adsorption capacity of 0.63 mmol/g at 25 °C and 1 bar (see Table 7). This behavior



may be due to the weak chemical interactions (physical interaction) between MCM-41 and CO<sub>2</sub> gas molecules because the existing hydroxyl groups are not capable of forming interactions or lack/missing of adsorption sites for CO<sub>2</sub> [96]. Apart from the above, Son et al. [96] prepared the KIT-6, SBA-15, SBA-16, MCM-48 and MCM-41 and their textural properties of the materials are tabulated in Table 7. Pore size of mesoporous materials are varied in the descending order of KIT-6 > SBA-15 > SBA-16 > MCM-48 > MCM-41. According to the aforementioned data, KIT-6 exhibits the largest pore volume among the other sorbents. These combined features of large pore size and large pore volume would enable KIT-6 to better accommodate the bulky polyethyleneimine (PEI) with little hindrance and allow higher loadings inside silica particles than other silica supported materials. Besides, Zeleňák and co-workers prepared three mesoporous silica materials with different pore sizes (3.3 nm MCM-41; 3.8 nm SBA-12; 7.1 nm SBA-15) [97]. During their studies, amine functionalization was investigated with the effect of pore size and pore architecture on CO<sub>2</sub> sorption. According to the reported data, SBA-15 showed the highest CO<sub>2</sub> adsorption of 1.5 mmol/g. This may be due to the highest amine surface density in SBA-15 [97].

Lashaki and Sayari [98] also investigated the impact of the support pore structure on the CO<sub>2</sub> adsorption performance of SBA-15 silica. In this study, SBA-15 silica supports are used to obtain different pore sizes and intra-wall pore volumes. These materials were functionalized further with triamine through dry and wet grafting. CO<sub>2</sub> sorption measurements showed the positive impact of support with large pore size and high intra wall pore volume on adsorptive properties, with the former being dominant. Large pore volume influenced to load more amine groups, CO<sub>2</sub> uptakes and CO<sub>2</sub>/N<sub>2</sub> ratios and faster kinetics. When the intra-wall pore volume decreased by 53%, it caused a reduction of CO<sub>2</sub> uptake capacity up to 63% and CO<sub>2</sub>/ N<sub>2</sub> ratios up to 62% and slower adsorption kinetics. Also, it was inferred that, large pore size and/or high intra-wall pore volume of the support improved the adsorptive properties via enhanced amine accessibility [98].

**Table 6.** The textural properties and CO<sub>2</sub> absorption capacity of different types of ordered mesoporous silica materials.

Types of mesoporous silica	Structure	Silica Source	Surfactant/ Block co- polymer	BET Specific surface area (m <sup>2</sup> /g)	Pore volume (cm <sup>3</sup> /g)	Pore size (nm)	Adsorption capacity (mmol/g)	Adsorption Conditions		Ref.
								Temp. (°C)	Pressure (bar)	
KIT-5	3D-cubic	TEOS	Pluronic P123	711	1.05	8.04	0.48	30	1	[99]
KIT-6	3D-cubic	TEOS	Pluronic P123	895	1.22	6.0	-	-	-	[96]
MCM - 41	Hexagonal	Na <sub>2</sub> SiO <sub>3</sub>	CTAB	994	1.00	3.03	0.63	25	1	[95]
		Na <sub>2</sub> SiO <sub>3</sub>	CTAB	993	1.00	3.1	0.63	25	1	[100]
		Na <sub>2</sub> SiO <sub>3</sub>	CTAB	980	0.92	4.08				[92]
MCM 48	Cubic	SiO <sub>2</sub>	CTAB	1287	1.1	3.5		25	1	[101]
SBA-15	2D hexagonal	TEOS	P123	1254	2.44	11.4	-	-	-	[102]
SBA-16	Cubic cage	TEOS	Pluronic F127	736	0.75	4.1	-	-	-	[96]
SNS		TEOS	Pluronic F127	394	0.10	21.1	2.06	25	1	[103]
SNT		TEOS	Pluronic F127	319	0.07	26.0	2.46	25	1	[103]

where CTAB: cetyltrimethylammoniumbromide and hexadecyltrimethylammoniumbromide, F127: tri-block copolymer F127, Na<sub>2</sub>SiO<sub>3</sub>: sodium silicate, P123: triblock copolymer (Pluronic P123), SiO<sub>2</sub>: silica, SNS: silica nano spheres, SNT: silica nano tube, TEOS: tetraethyl orthosilicate.

**Table 7.** CO<sub>2</sub> adsorption capacities and structural properties of amine functionalized silica-based adsorbents.

Silica-based sorbent	Amine types	CO <sub>2</sub> adsorption performance capacity (mmol/g)	Conditions		BET Specific surface area (m <sup>2</sup> /g)	Pore volume (cm <sup>3</sup> /g)	Pore size (nm)	Preparation methods	Ref
			Tempera ture (°C)	Pressure (bar)					
DWSNT	-	0.1	25		83	0.58		Immobilization	[126]
DWSNT	APTMS	1.0	25		112	0.72		Immobilization	[126]
DWSNT	MAPTMS	1.5	25		114	0.79		Immobilization	[126]
DWSNT	DEAPTMS	1.8	25		68.9	0.49		Immobilization	[126]
DWSNT	AEAPTMS	2.25	25		60.9	0.45		Immobilization	[126]

<b>HAS</b>	Aziridines	3.25	25		71	5	0.15		[127]
<b>HPS</b>	PEI	2.44	75	1	0.5	0.009		Impregnation	[128]
<b>HVMCM-41</b>	PEHA	4.07	105	1				Impregnation	[125]
<b>KIT-6</b>	PEHA	4.48	105	1				Impregnation	[125]
<b>MCM-41</b>	EDA	1.19	35					Impregnation	[129]
<b>MCM-41</b>	DETA	1.43	35					Impregnation	[129]
<b>MCM-41</b>	TEPA	1.96	35					Impregnation	[129]
<b>MCM-41</b>	PEHA	2.34	35					Impregnation	[129]
<b>MCM-41</b>	MEA (3%)	11.39	25		426	0.42	3.12	Impregnation	[130]
<b>MCM-41</b>	PEI	0.39	40	0.15	443	0.340	2.95	Impregnation	[49]
<b>MCM-41</b>	PEI	0.22	75	1	590	1.4	13.6	Impregnation	[122]
<b>MCM-41</b>	PEI Aziridine	0.98	75	1				In-situ grafted polymerization	[131]
<b>MCM-41</b>	APTS	94	25	1	10	0.01		Grafting	[116]
<b>MCM-41</b>	APTS	2.48	20	1	17	0.04	20.1	Grafting	[133]
<b>MCM-41</b>	PEHA	4.5	105	1				Impregnation	[122]
<b>MCM-41</b>	MEA	0.89	25	1	19	0.82		Impregnation	[100]
<b>MCM-41</b>	DEA	0.80	25	1	13	0.07		Impregnation	[100]
<b>MCM-41</b>	TEA	0.63	25	1	213	0.17		Impregnation	[100]
<b>MCM-41</b>	Branched PEI	1.08	100	1	6	0	-	Impregnation	[95]
<b>MCM-41</b>	Branched PEI	0.79	100	1	12	0.04	-	Impregnation	[95]
<b>MCM-41</b>	Branched PEI – (30 wt%)	0.70	100	1	80	0.14	-	Impregnation	[95]
<b>MCM-41</b>	Branched PEI	28	100	1	104	0.12	2.05	Impregnation	[95]
<b>MCM-41</b>	Branched PEI	17.5	100	1	291	0.17	2.05	Impregnation	[95]
<b>MCM-41</b>	TEPA	1.24	25	1	11	0.05	1.8	Impregnation	[134]
<b>MCM-48</b>	APTES	0.62	25	1.01	1072	0.52	2.9	Grafting	[101]
<b>MCM-48</b>	TRI	0.46	25	1.01	698	0.39	2.6	Grafting	[101]
<b>MCM-48</b>	TRI	0.44	25	1.01	463	0.23	2.5	Grafting	[101]
<b>MSiNTs</b>	PEI	2.75	92		52.4	0.17	12.4	Impregnation	[135]
<b>OMS</b>	PEI	1.4	25		352	0.79		Grafting	[122]

<b>SAB-15</b>	PEHA	4.0	105	1				Impregnation	[125]
<b>SBA-15</b>	PEI	0.65	25		683	1.19	8.5	Impregnation	[124]
<b>SBA-15</b>	PEI/Zr4	1.34	25		642	1.08	8.6	Impregnation	[124]
<b>SBA-15</b>	PEI/Zr7	1.56	25		674	1.23	9.5	Impregnation	[124]
<b>SBA-15</b>	PEI/Zr14	1.41	25		601	0.69	7.0	Impregnation	[124]
<b>SBA-15</b>	PEI/Ti1.4	0.24	25		510	0.39	4.4	Impregnation	[124]
<b>SBA-15</b>	NH <sub>2</sub> OH	1.65	25	1	435.6	0.54	6.85	Grafting	[136]
<b>SBA-15</b>	APTMS	1.46	25	0.15	82	0.16	5	Grafting	[137]
<b>SBA-15</b>	TEPA	2.45	70		5	0.03		Grafting	[102]
<b>SBA-15</b>	AMP	1.79	70		372	0.21		Grafting	[122]
<b>SBA-15 (0.2µm)</b>	PEI	5.84	100	1	590	1.44	13.6	Impregnation	[122]
<b>SBA-15 (1.5µm)</b>	PEI	-	100	1	746	0.80	7.2	Impregnation	[122]
<b>SBA-15 (25µm)</b>	PEI	5.81	100	1	580	0.95	10.5	Impregnation	[122]
<b>SiO<sub>2</sub></b>	APTES	4.3	30		67	0.51		In-situ polymerization	[29]
<b>SiO<sub>2</sub></b>	AEAPTMS	5.7	30		45	0.37		In-situ polymerization	[29]
<b>SiO<sub>2</sub></b>	TRI	5.6	30		25	0.22		In-situ polymerization	[29]
<b>SiO<sub>2</sub></b>	APTES	0.5	30		216	1.11		Grafting	[29]
<b>SiO<sub>2</sub></b>	AEAPTMS	0.3	30		206	1.10		Grafting	[29]
<b>SiO<sub>2</sub></b>	TRI	0.8	30		172	0.99		Grafting	[29]
<b>SMCM-41</b>	MEA	10.40	25		405	0.39	3.01	Impregnation	[130]
<b>SBA-15</b>	TEPA	4.5	75	1	121.1	0.327		Impregnation	[138]
<b>MPSM</b>	TEA	4.27	75	1	34	0.08	9.5	Impregnation	[50]
<b>MCM-41</b>	TRI	1.74	25	0.05	678.3	1.47		Grafting	[139]
<b>MCM-41</b>	APTES	1.20	30	1	1045.21	2.59	30	Grafting	[140]
<b>MCM-41</b>	PEI	0.98	30	1	6.6	0.01	0.8	Grafting	[141]
<b>MCM-41</b>	PEI	4.68	45	1	894	1.28	5.1	Grafting	[118]
<b>MCM-41</b>	PEI	2.92	50	0.1	508	0.98	2.54	Impregnation	[142]
<b>MCM-41</b>	TEPA	2.25	50	0.1	431	0.83	2.21	Impregnation	[142]
<b>MCM-41- KOH</b>	PEI-	3.38	50	0.1	391	1.08	2.33	Impregnation	[142]
<b>MCM-41- Ca(OH)<sub>2</sub></b>	PEI-	3.81	50	0.1	411	1.12	2.50	Impregnation	[142]

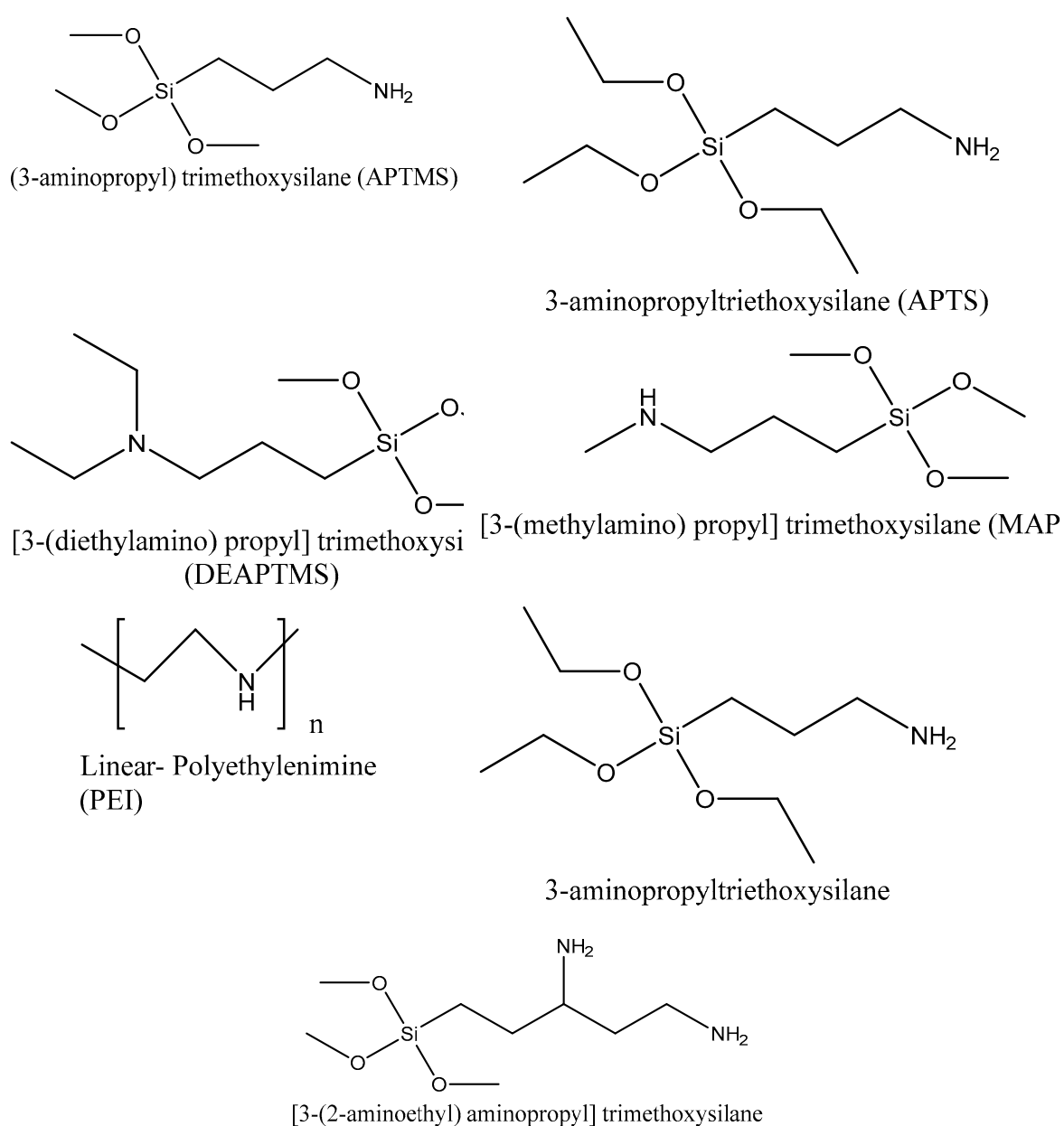
MCM-41- CsOH	PEI-	5.02	50	0.1	306	0.91	2.14	Impregnation	[142]
MCM-41- KOH	TEPA-	3.93	50	0.1	322	0.97	2.15	Impregnation	[142]
MCM-41- Ca(OH) <sub>2</sub>	TEPA-	3.76	50	0.1	405	0.94	2.31	Impregnation	[142]
PET- CsOH	TEPA-	5.42	50	0.1	293	0.97	2.61	Impregnation	[142]
MCM 48	PEI	1.09	80	0.24	79.3	0.02	1.68	Impregnation	[143]
MCM-41	PEI	1.23	80	0.24	59.1	0.02	1.80	Impregnation	[143]
SBA-15	PEI	1.07	80	0.24	62.1	0.01	5.2	Impregnation	[143]
SBA-15	PEI	1.77	0	1	783	0.03	7.0	Impregnation	[144]
SBA-15	PEI	1.26	45	0.15	399	0.79	8.2	Impregnation	[145]
MCM 41	PEI	3.53	25	1	24	0.012		Impregnation	[146]
MCM 41	APTS	2.41	25	1	736	0.37		Grafting	[146]
SBA-15	PEI	1.84	25	1.2	195	0.39	7.0	Grafting	[147]
SBA-15- APES		1.78	25	1.2	190	0.37	7.2	Grafting	[147]
SBA-15- APES	PEI	1.54	25	1.2	24	0.21	2.7	Grafting	[147]
OMS	PEI	2.43	25	1.2	167	0.33	7.6	Grafting	[147]
OMS- APES		3.03	25	1.2	180	0.37	7.2	Grafting	[147]
OMS- APES	PEI	1.18	25	1.2	39	0.18	2.3	Grafting	[147]
OMS- NCC	Amidoxime	5.54	120	1	315	0.69	9.3		[148]
MPS-MCC*		2.41	120		302	0.44	7.0		[149]
MPS-MCC**		3.85	120		285	0.40	6.7		[149]
OMS- MgO		4.71	120	1	261	0.48	7.25		[150]
OMS-CaO		3.85	120	1	163	0.25	6.76		[150]
SiO <sub>2</sub> - Al <sub>2</sub> O <sub>3</sub>	APTS	2.64	25	1	740	1.24	5.1	Grafting	[151]
SiO <sub>2</sub> - Al(NO <sub>3</sub> ) <sub>3</sub>	APTS	0.78	25	1	319	0.63	2.9	Grafting	[151]
OMS-Ti		0.81	25	1	487				[90]
MSiNTs	APTES	2.87	25	1.2	293	0.79	22	Grafting	[103]
SNS	APTES	2.13	25	1.2	210	0.31	19.6	Grafting	[103]
Al(NO <sub>3</sub> ) <sub>3</sub>	AP	0.98	25	1	359	0.62	10.0		[152]
OMS-Al-Zr		2.60	60	1	441	0.61	6.9		[153]

Where, \*\* MCC- mesoporous silica with amidoxime functionalities, \*MCC-mesoporous silica with cyanopropyl groups, APTMS: 3-[2-(2-aminoethylamino)ethylamino]propyltrimethoxysilane, AEAPTMS: [3-(2-aminoethyl) aminopropyl]trimethoxysilane, AMP: 2-amino-2-methyl-1-propanol, AP: 3-

aminopropyltriethoxysilane, APTMS: (3-aminopropyl) trimethoxysilane, APTS: 3-aminopropyltrimethoxysilane, DEA: diethanolamine, DEAPTMS: [3-(diethylamino) propyl]trimethoxysilane, DETA: diethylenetriamine, DWSNT: double-walled silica nano tube, EDA: ethylenediamine, HPS: Hierarchically porous silica, MAPTMS: [3-(methylamino) propyl]trimethoxysilane, MCC: microcrystalline cellulose, MEA: monoethanolamine, MPSM: monodispersed porous silica microspheres, MSiNTs: mesoporous silica nanotubes, NCC: nanocrystalline cellulose, OMS: ordered mesoporous organosilica, OMS: Oxide-templated silica monoliths, PEHA: pentaethylenhexamine, PEI: polyethylenimine, SNS: silica nano spheres, TEA: triethanolamine, TEPA: tetraethylenepentamine, TRI: 3-[2-(2-Aminoethylamino)ethylamino]propyltrimethoxysilane.

## 5. Chemisorbents (amine functionalized Si-based materials) - application at low and high temperature CO<sub>2</sub> sorption

In the physisorption process, CO<sub>2</sub> molecules attach to the pore walls through the weak Van der Waals and pole–pole interactions [104]. However, the unmatched pore size of the mesoporous silica and small diameter of CO<sub>2</sub> gas molecule causes low CO<sub>2</sub> adsorption capacities. The heat of adsorption of physisorption process ranges from -25 to -40 kJ/mol [105], which is approximately closer to the heat of sublimation [106]. Recently, it has been reported about the mesoporous silica materials with improved CO<sub>2</sub> sorption capacity with amine functionalization [107]. However, the adsorption capacity of CO<sub>2</sub> depends on the nature of the amine groups and the spacing between the amino silanes [108]. Figure 7 represents the different types of amino silanes- and polymer containing amino groups used during the functionalization of mesoporous silicas for enhanced adsorption or separation.





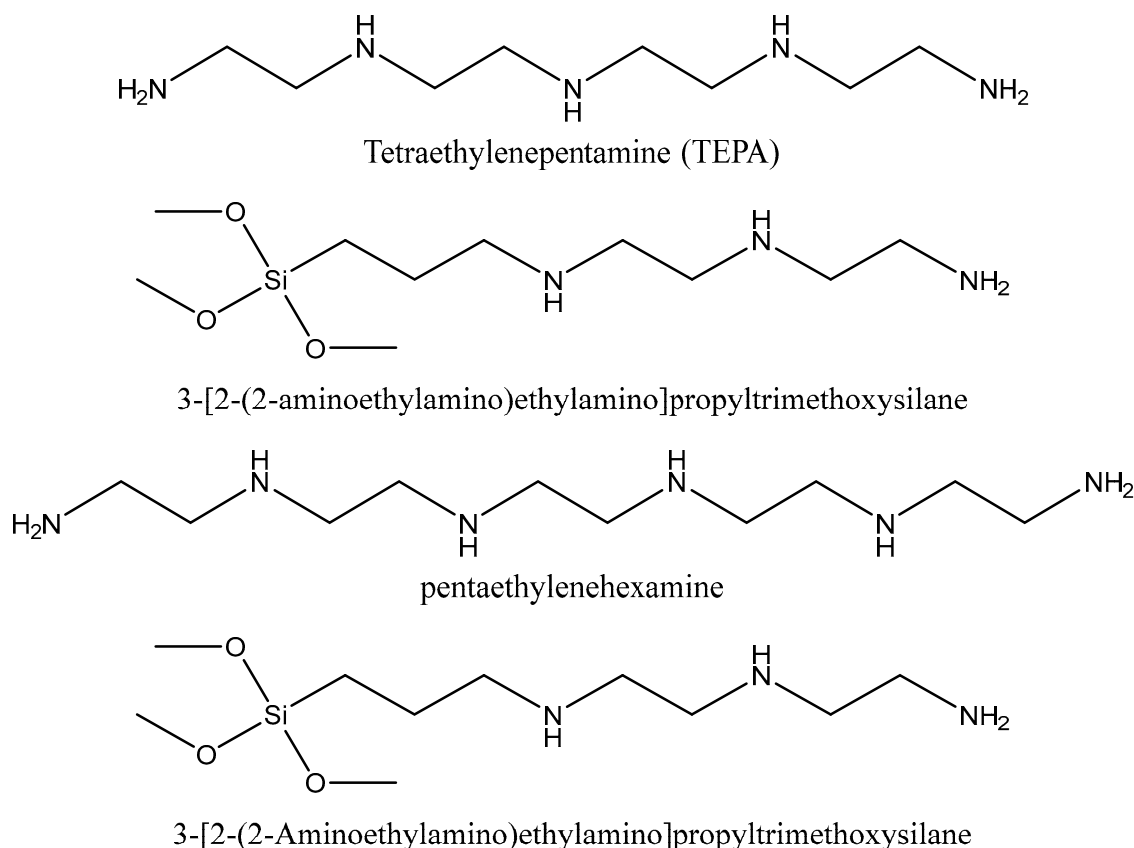


**Figure 7.** Various amino silane- and polymer-containing amino groups used in the functionalization of mesoporous silicas.

### 5.1. Synthesis procedures

Recently, the improvement of amine-based adsorbents was conducted by three approaches: the preparation of supports with high amine loadings, use of amine with high nitrogen content and use of effective methods for amine introduction [44]. Synthesis methods of amine functionalized silica materials have three main pathways including impregnation, grafting, and in situ polymerization as shown in Figure 8.

In impregnation, amines are physically trapped in the pores of silica materials as shown in Figure 8. Moreover, performance of amine-silica adsorbents is influenced by the pore structure of silicas. However, Chen et al. [109] and Chen et al. [110] have reported that the  $\text{CO}_2$  adsorption capacities follow the order of decreasing pore diameter. Moreover, surfactant, surface functional groups, amine types and heteroatom incorporation affect the impregnation process [54]. In this method, the amine loading is affected by the total pore volume of the silica materials and the density of the amine. Moreover, if the amount of amine exceeds the capacity of the support, the amine species will agglomerate. The main advantage of this method is its simplicity and involvement of its mild synthesis procedure. Further, large amount of amine species is cooperated with mesoporous silica due to the large pore volume of the porous silica materials [111].

Grafting occurs between an aminosilane with silica to introduce amine groups as shown in Figure 8 where the amines are grafted on the silica surface via covalent bonds [112]. Mainly, three methods are used for the grafting of amine onto a silica support which are, post-synthesis grafting, direct synthesis by co-condensation (one pot synthesis), and anionic template synthesis [113]. In a typical process, silica is dispersed in a solvent and then amino silanes were added and the mixture is heated under reflux. However, the amount of amine incorporated is related to the number of hydroxyl groups on the silica surface [111]. In-situ polymerization is another promising method for

functionalizing porous silica such as hyperbranched aminosilica (HAS). This category of supported sorbents can be considered as a hybrid of the grafting and impregnation [114].

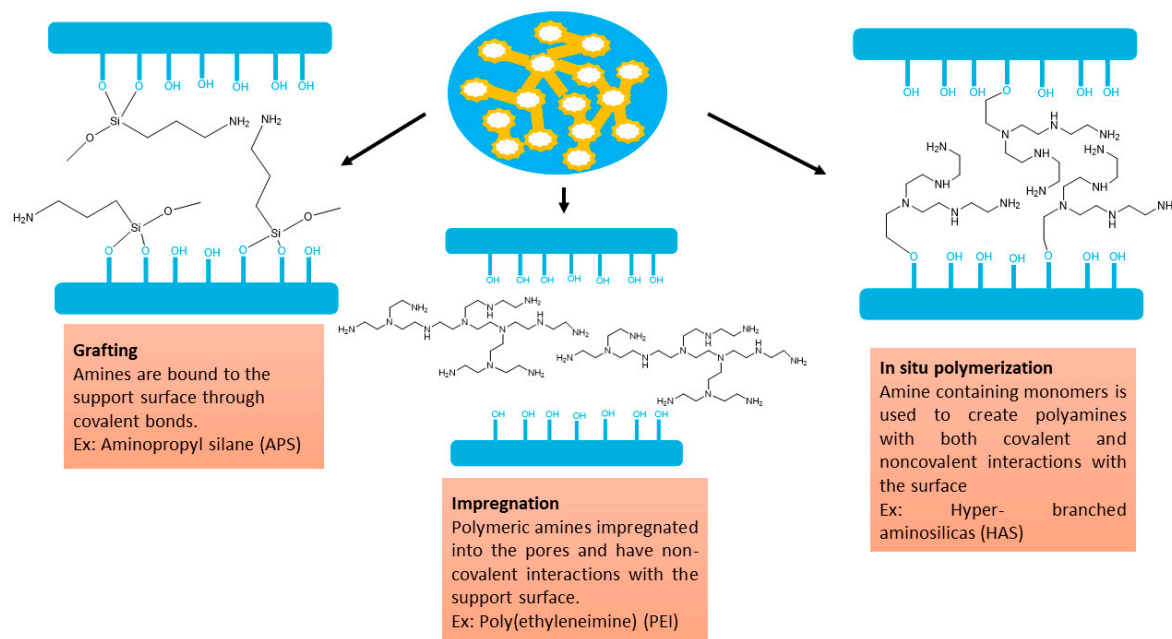


**Figure 8.** Different types of synthesis processes of amine-functionalized silica materials (Schematic shows supported amines (yellow) in the pores (blue)) (Reprinted with permission from Bollini et al. [115]).

In contrast, toxic solvents (toluene) are used for grafting process. Therefore, because of the simplicity, low cost, environmental friendliness, and convenience for large scale production, the impregnating technique is widely used [116]. However, in order to overcome the challenges caused by grafting, researchers have recently investigated the aminosilane gas-phase grafting and supercritical fluid impregnation [117].

Supercritical fluid impregnation is considered to be one of the most effective, simple and reproducible methods for producing homogeneous, covalently bonded and high-density silane [117]. López-Aranguren et al. [117] synthesized functionalized silica via supercritical CO<sub>2</sub> grafting of aminosilanes. For this study, silica gels (4.1 and 8.8 nm pore diameter), mesoporous silica MCM-41 (3.8 nm pore diameter) and mono- and di-aminotrialkoxysilane were chosen.

The method called double functionalization of mesoporous materials is also widely used in recent years. Several groups have prepared amine–silica composites using a double-functionalization method [118–120]. In those studies, impregnation and grafting were used to improve the CO<sub>2</sub> uptake [118].

## 5.2. Comparison of adsorption capacities

Nigar et al. [101] have synthesized the ordered mesoporous (MCM-48) silica with different silane molecules including 3-triethoxysilylpropylamine, 3-(2-aminoethylamino) propyl] trimethoxysilane and 2-[2-(3-trimethoxysilylpropylamino)ethylamino]ethylamine. Herein, silane groups were covalently bound with the silica groups as shown in Figure 9. The functionalization caused the reduction of the surface area and the pore volume compared to the non-functionalized MCM-48 (1287 m<sup>2</sup>/g and 1.1 cm<sup>3</sup>/g) (see Table 7). Most importantly, it is clearly seen that, with the increment of number amine groups in silane molecules caused a decrease of CO<sub>2</sub> absorption capacity governed through chemisorption [101].

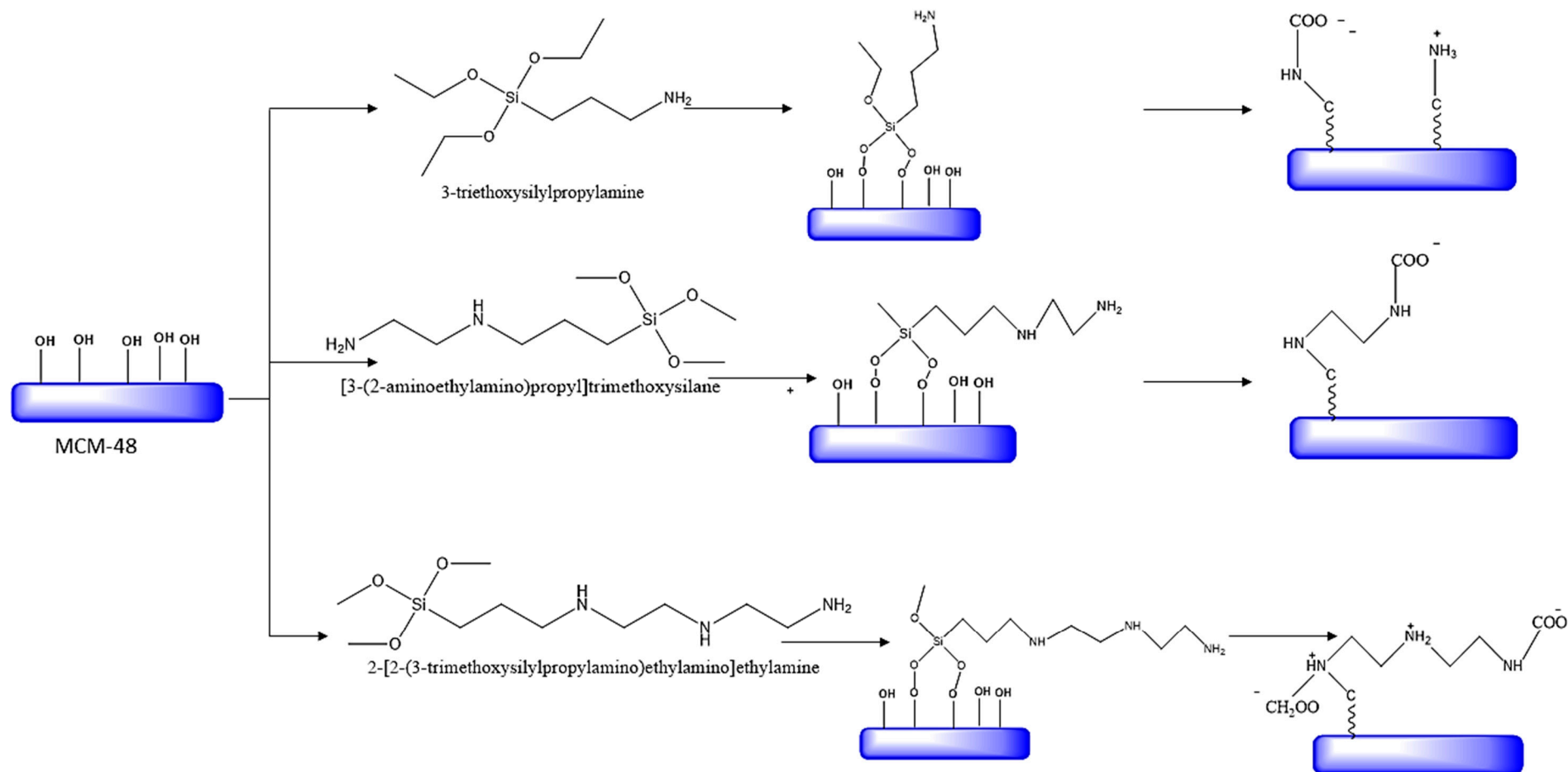


**Figure 9.** Schematic representation of the covalent bonding through the alkyl-silyl linkages and formation of carbamates (Reprinted with permission from Nigar et al..

Moreover, Park et al. [29] synthesized functionalized silica using the silane molecules as similar to the studies conducted by Niger et al. [101]. However, they have compared in-situ polymerization and grafting. According to the data reported here, (see Table 7) it is shown that, sorbent prepared through in-situ polymerization show enhanced CO<sub>2</sub> adsorption capacity. Ahmed et al. [95] reported a detailed study about functionalization of mesoporous Si-MCM-41 with different loadings of PEI. According to that, with the increment of PEI loading, the CO<sub>2</sub> adsorption capacity increased (see Table 7). This behavior is suggested as the branched PEI exhibits high density of amino groups as potential CO<sub>2</sub>-affinity sites and the hierarchical mesoporous structure of Si-MCM-41 makes these sites accessible by improving the dispersion of PEI [121].

Gargiulo and co-workers reported the effect of temperature on CO<sub>2</sub> adsorption capacity on SBA-15 and PEI. CO<sub>2</sub> adsorption were evaluated at 25, 40, 55, and 75 °C temperatures [122]. According to the experimental data, a significant dependence of the CO<sub>2</sub> adsorption capacity on temperature was observed (Table 7). The effect of pore dimension on CO<sub>2</sub> adsorption over amine-modified mesoporous silicas were reported by Heydari-Gorji et al. [102]. The pore lengths of the silica supports were 25, 1.5, and 0.2 µm. It showed that the small pore size of silica materials exhibited the highest adsorption capacities which are caused by enhanced amine accessibility inside the pores. Heydari-Gorji and Sayari, [123] investigated the PEI impregnation for CO<sub>2</sub> removal applications. It demonstrated that PEI functionalized silica materials were thermally stable at mild temperatures. On the contrary, the adsorbent was stable after long-term exposure to gas mixtures (CO<sub>2</sub> and O<sub>2</sub>) due to the presence of CO<sub>2</sub>. Amine groups are protected from oxygen attack, because of rapid formation of carbamate and bicarbonate structures. Kuwahara et al. [124] synthesized poly(ethyleneimine)/silica composite adsorbents by incorporating zirconium (Zr) into the silica support. According to the results observed, Zr sites show an increase in the CO<sub>2</sub> adsorbent capacity (see table 7), regenerability, and stability.

Apart from that, Kishor and Ghoshal [125] investigated the effect of the structural parameters of the silicas and amine-functionalized silicas such as pore size, pore-volume, and surface area on the CO<sub>2</sub> sorption capacity. For this study, various silicas such as KIT-6, MCM-41, SBA-15, and HV-MCM-41 were used. Wet impregnation method was used by them to prepare the pentaethylenhexamine (PEHA) functionalized silicas. The CO<sub>2</sub> capture capacities of the amine-functionalized silicas were measured at 105 °C and 1 bar pressure conditions (see Table 7). The KIT-6 showed the highest CO<sub>2</sub> capture capacity of 4.48 mmol/g of CO<sub>2</sub> at 105 °C and 1 bar pressure) among all the sorbents investigated (MCM-41 < HVMCM-41 < SBA-15 < KIT-6). Furthermore, KIT-6 showed enhanced amine density distribution due to large pore volume. All the other silica sorbents remained stable up to ten adsorption-desorption cycles.

In contrast, Sim and co-workers [147] have studied the CO<sub>2</sub> absorption capacity of the silica-based composites papered using SBA-15 and organosilica as silica precursors and N-[3-(trimethoxysilyl)propyl]ethylenediamine as an aminosilane precursor. Herein, PEI was grafted to the silica composites. Results exhibited that, organosilica composites sample (see Table 7) showed the highest CO<sub>2</sub> adsorption capacity, selectivity and reproducibility. Another silica composite was prepared by Dassanayake et al. [148] using nano-crystalline cellulose. According to the reported data, nano-crystalline cellulose mesoporous silica showed high CO<sub>2</sub> absorption capacity (see Table 7), recyclability and thermal stability. Authors further reported that, synthesis process is relatively cheap and simple compared to other composites studied. Gunathilake et al., [149] have prepared the microcrystalline cellulose (MCC) mesoporous silica composites. Prepared composites-based sorbent materials showed biocompatibility, biodegradability, non-toxicity, cyclic stability, and thermal and mechanical stability. Herein, two MCC-mesoporous silica composites were prepared as follows; MCC-mesoporous silica with cyanopropyl groups were first synthesized and then cyanopropyl groups were converted into the amidoxime functionalities. CO<sub>2</sub> adsorption was evaluated at 25 and 120 °C. According to the results, MCC- mesoporous silica with amidoxime functionalities exhibited the highest absorption capacity (see Table 7) at 120 °C due to the oxime and amine groups in amidoxime functionality and hydroxyl groups in MCC which serve as active sites while assuring highest CO<sub>2</sub> adsorption.

On the other hand, Rao et al. [146] determined the effect of impregnation and grafting of the amine-functionalized MCM-41. The results exhibited that (Table 7) grafted sorbents showed highest thermal stability than the impregnation ones. They concluded that, adsorbents modified by impregnation showed higher amine-loading efficiencies and thus higher CO<sub>2</sub> adsorption capacities whereas those prepared by the grafting had better thermal and cyclic stability.

Moreover, Tang and co-workers have investigated the effect of inorganic alkalis such as (KOH, Ca(OH)<sub>2</sub> and CsOH) on the CO<sub>2</sub> absorption capacity [142]. The results showed that all the three kinds of inorganic alkali-containing adsorbents exhibit higher CO<sub>2</sub> adsorption capacities than tetraethylenepentamine (TEPA) and PEI modified samples (see Table 7). This may be due to the introduction of inorganic alkali which changes the chemical adsorption mechanism between adsorbate-CO<sub>2</sub> and the adsorbent surface due to the increase of hydroxyl groups. Also, they reported that CO<sub>2</sub> adsorption capacities have a linear dependence relationship with the amounts of alkali adsorbents. Apart from that, Gunathilake and Jaroniec [150] reported the incorporation of magnesium oxide and calcium oxide into mesoporous silica surface (OMS) and applied those materials for CO<sub>2</sub> sorption at ambient and elevated temperatures. The materials were synthesized using sol-gel method. However, the resulted composite sorbents performed relatively high adsorption capacities (see Table 7). It suggested that MgO and CaO caused an increase of physisorption of CO<sub>2</sub> via microspores plus chemisorption via hydroxyl groups. Those synthesized CaO-SiO<sub>2</sub> and MgO-SiO<sub>2</sub> composites showed high surface area, basic surface properties and high thermal and chemical stability.

Alumina materials also possess high surface area, porosity, and thermal and mechanical stability. Therefore, recently, researchers have used the amine-grafted mesoporous silica and impregnated alumina as solid sorbents for CO<sub>2</sub> capture [151]. Alumina-based materials for CO<sub>2</sub> capture includes basic Al<sub>2</sub>O<sub>3</sub>, amine-impregnated or amine-modified mesoporous Al<sub>2</sub>O<sub>3</sub> and Al<sub>2</sub>O<sub>3</sub>-organosilica [151]. Gunathilake et al. [151] synthesized Al<sub>2</sub>O<sub>3</sub>-organosilica by introducing three different silica precursors such as tris [3-(trimethoxysilyl)propyl] isocyanurate (ICS), 1,4-bis(triethoxysilyl)benzene (BTEB), and bis(triethoxysilyl)ethane (BTEE). In this study, two alumina precursors aluminum nitrate nanohydrate and aluminum isopropoxide were used whereas grafting of amine groups was performed using 3-aminopropyltriethoxysilane (APTS). According to the results obtained of this study, SiO<sub>2</sub>- Al<sub>2</sub>O<sub>3</sub> showed the highest absorption capacity (Table 7) and the adsorption properties of the materials depend on the surface area of the sample, alumina precursor, and structure and functionality of the organosilica bridging group. Besides, Choi et al. [154] used epoxy-functionalized PEI for the synthesis of CO<sub>2</sub> sorbents. According to the reported data, epoxy-functionalized PEI exhibited a CO<sub>2</sub> capacity of 2.2 mmol/g at 120 °C and 100% regeneration capability at similar temperature. This can be attributed to the heat resistant properties of epoxy butane which enhanced the CO<sub>2</sub> capture capacity and thermal stability of the silica-epoxy-PEI sorbent.

However, according to the reported data by Hu et al. [155], Li<sub>4</sub>SiO<sub>4</sub> exhibited attractive prospects for CO<sub>2</sub> capture and the main advantage is high CO<sub>2</sub> sorption capacity (theoretical sorption capacity of 0.367 g CO<sub>2</sub>/g sorbent) and lower regeneration temperature (< 750 °C) in comparison with other reported materials such as CaO which requires a regeneration temperature of over 900 °C [155].

### 5.3. Sorbent selectivity, regeneration and stability in the cyclic CO<sub>2</sub> adsorption-desorption runs

During industrial applications, high adsorption capacity along with good regenerability of the sorbents in the cyclic adsorption-desorption process is of vital importance [119]. The practical application of an adsorbent requires high sorption capacity, easy regeneration, stability in normal atmosphere, as well as stable performance during cyclic use for a long-term operation.

For instance, Ahmed et al. [95] reported a detailed study about functionalization of mesoporous MCM-41 with different loadings of polyethylenimine (PEI). In this study, the selectivity measurement was conducted for CO<sub>2</sub> over N<sub>2</sub> and H<sub>2</sub>. According to the results obtained, the adsorption capacities of N<sub>2</sub> and H<sub>2</sub> on 50 wt% PEI-Si-MCM- 41 were obtained as 3.89 mg/g and 6.51 mg/g, respectively (see

Table 8). Table 8 represents the summary of gas selectivity values of previous studies done for porous SiO<sub>2</sub>.

**Table 8.** Summary of gas selectivity values of previous studies done for porous SiO<sub>2</sub>.

Porous SiO <sub>2</sub> material	Gas mixture	Selectivity value	Pressure (bar)	Temperature (°C)	Reference
PEI-MCM-41	CO <sub>2</sub> , N <sub>2</sub> and H <sub>2</sub>	25.56	1	100	[95]
SBA-15	CO <sub>2</sub> /N <sub>2</sub>	123	1	25	[156]
SBA-15 (calcination)	CO <sub>2</sub> /N <sub>2</sub>	55	1	25	[156]
Mesoporous chitosan-SiO <sub>2</sub> nanoparticles	-	15.46	1	25	[157]
hydrophobic microporous high-silica zeolites	CH <sub>4</sub> :N <sub>2</sub> = 50%:50%	36.5	1	25	[158]
Hollow silica spherical particles (HSSP)	CO <sub>2</sub> /N <sub>2</sub>	8.5	4	25	[159]
microporous silica xerogel	CO <sub>2</sub> /CH <sub>4</sub>	60	6	25	[160]
Silica based xerogels	C <sub>2</sub> H <sub>4</sub> /C <sub>2</sub> H <sub>6</sub>	20	6	25	[160]

Wang et al. [156] prepared SBA-15 using two template removal methods which are, silica: ethanol extraction and conventional high-temperature calcination. Then, the resulted silicas were subjected to amine (3-aminopropyl) grafting and studied for their CO<sub>2</sub> adsorption properties. The aim of this study was to increase the surface silanol density, and hence the grafted amine loading leads directly to increased CO<sub>2</sub> adsorption capacity and CO<sub>2</sub>/N<sub>2</sub> selectivity. According to the reported data, CO<sub>2</sub>/N<sub>2</sub> selectivity changed from 46 to 13 (see Table 8) and these results ensured that solvent extraction also leads to an enhancement in CO<sub>2</sub>/N<sub>2</sub> selectivity. Also, the authors performed a test to measure the stability of amine-SBA-15 (solvent extracted). According to the results, after each adsorption step, amine-SBA-15 (solvent extracted) was regenerated under a vacuum.

In industrial applications of adsorbents, it is important to remain stable during cyclic operations. This section summarizes the reported studies on sorbent regeneration and stability in cyclic CO<sub>2</sub> adsorption –desorption runs by amine–silica composites and reported data is tabulated in Table 9. The regeneration of the amine-impregnated and grafted silica composites was mainly conducted by pressure and temperature swing adsorptions. Typically, the sorbent was regenerated at a temperature of 50 ~120 °C in N<sub>2</sub>, He, or Ar flow. As depicted in Table 9, the amine-impregnated silica composites show loss of CO<sub>2</sub> capture capacity in the cyclic CO<sub>2</sub> sorption –desorption runs, due to amine leaching from the silica surface and degradation [112]. Amine leaching is closely related to the amine types introduced and the operation temperature, while the degradation of amine is related to the operation temperature and gas atmosphere [111].

Therefore, Guo et al. [128] have conducted the adsorption/desorption cycles for hierarchically porous silica (HPS) grafted PEI at 75 °C. In this experiment, the modelled flue gas flow rate was maintained at 70 mL/min and the CO<sub>2</sub> partial pressure was maintained at 1 bar. According to the data, adsorption capacities are similar in eight adsorption/desorption cycles, showing that the aforementioned sorbents have good stability and regenerability.



Wang et al. [119] investigated the regenerability of the amine modified MCM-41 (MCM-41-TEPA and MCM-41-AMP). Authors have conducted fifteen cycles to verify the regenerability. According to the reported data, after fifteen cycles, the adsorption capacity decreased from 3.01 mmol/g to 2.88 mmol/g and it was shown that both sorbents showed good regenerability. This may be due to the hydrogen-bonding interactions among TEPA, AMP and MCM-41, TEPA.

Kishor and Ghoshal [125] measured the stability of the pentaethylenhexamine (PEHA) impregnated KIT-6. The sorbent was aged for 6 months, and its adsorption performance was explored at 90–105 °C. According to the results, PEHA impregnated KIT-6 showed sorption capacities of 4.0 and 4.3 mol CO<sub>2</sub>/ kg at 90 and 105 °C at 1 bar even after 6 months. Also, the sorption performance of adsorbent was tested for ten consecutive adsorption/desorption cycles. The sorption capacity of the sorbent decreased by less than 4% in 90–105 °C at 1 bar without any structural degradation. Moreover, the results exhibited that, PEHA impregnated KIT-6 have better sorption performance than those of earlier reported adsorbents, except for silica aerogel.

Liu and co-workers carried out regeneration test for zeolite-mesoporous silica-supported-amine hybrids sorbent [162]. According to the reported data, after 10 cycles, the adsorption capacity demonstrated almost no change, therefore, the sample performed a very stable cyclic adsorption-desorption performance. In contrast, López-Aranguren et al. [131] examined the regeneration of CO<sub>2</sub> from branched PEI - mesoporous silica.



**Table 9.** Summary of stability of silica-based adsorbent studied in past performance capacity.

Synthesis method	Type of silica-based sorbent	Amine type	Regeneration condition		Stability performance		References
			Temperature (°C)	Types of gas flow	No. of cycles (cyclic runs)	Capacity loss (%)	
Impregnated	MCM-41	PEHA	100	N <sub>2</sub>	15	Less than 1	[161]
	MCM-41	TEPA +AMP	100	N <sub>2</sub> for 60 min	15	4.32	[119]
	SBA-15	PEI-linear	100	Ar	12	13.5	[162]
	SBA-15	Acrylonitrile-modified TEPA	100	N <sub>2</sub>	12	1.1	[163]
	HMS	PEI-linear	75	N <sub>2</sub> for 100 min	4	1.6	[164]
	MCF	PEI- branched	115	Ar for 20 min	10	32	[165]
	MCF	PEI	100	H <sub>2</sub>	10	5	[166]
	MCF	Guanidinylated poly(allylamine)	120	He	5	17	[52]
	Fumed silica	PEI-linear	55	N <sub>2</sub> for 15min	180	Stable	[167]
	MCM-41	TEPA	100	N <sub>2</sub>	10	3.43	[168]
	Silica fume	Diisopropanolamine	50	N <sub>2</sub>	10	7	[169]
	Nano- SiO <sub>2</sub>	PEI- branched	120	N <sub>2</sub>	30	10.5	[170]
	Nano- SiO <sub>2</sub>	PEI- branched	120	N <sub>2</sub>	30	19.4	[171]
	Mesoporous-SiO <sub>2</sub>	APTS	120	Air for 30 min	11	4.3	[172]
	Porous SiO <sub>2</sub>	PEI	100	N <sub>2</sub> for 30 min	20	5	[173]
	Silica aerogel	TEPA	75	Ar for 20 min	10	3.9	[174]
	Porous SiO <sub>2</sub>	TEPA	75	He for 20 min	10	2	[175]

Grafting	SNT	PEI	110	N <sub>2</sub> for 40 min	10	3.3	[134]
	KCC-1- SiO <sub>2</sub>	TEPA	110	N <sub>2</sub>	21	1.2	[176]
	Mesoporous multilamellar SiO <sub>2</sub>	PEI	110	N <sub>2</sub>	10	3.7	[177]
	Silica aerogel	TEPA	80	Ar for 30 min	100	12	[176]
	Mesoporous SiO <sub>2</sub>	DEA	90	N <sub>2</sub>	10	12	[172]
	SBA-15	AP	90	Vacuum	10	1	[178]
	SBA-15	DEAPTMS	120	N <sub>2</sub> for 10 min	100	7.2	[179]
	MCM-48	2-[2-(3-trimethoxysilyl propylamino) ethylamino] ethylamine	-	N <sub>2</sub>	20	Stable	[100]
	KIT-6	APTES	120	He	10	Stable	[99]
	MCF	TRI	150	N <sub>2</sub> for 30 min	5	1.9	[180]
	HMS	APTS	110	N <sub>2</sub> for 180 min	3	Less than 1	[181]
	MCM-41	APTS	105	N <sub>2</sub> for 90 min	10	Stable	[117]

In this study, CO<sub>2</sub> adsorption/desorption cycles showed that the uptake measured in the first cycle was successfully maintained even after 20 cycles. Zhang et al. [177] examined the stability of the adsorbents based on linear PEI supported on silica. According to the reported data, the adsorbent maintained its adsorption capacity, but the adsorption capacity reduced by approximately 5.6% when the temperature was increased to 100 °C, which was attributed to amine leaching. Furthermore, Subagyono et al. [165] found that the branched PEI containing adsorbent showed a decrease in CO<sub>2</sub> adsorption –desorption capacity during cycling which is attributed to the by-product formation.

## 6. Technical Challenges and Future Trends

Facing financial and technical challenges are the main barriers for CO<sub>2</sub> commercial utilization. From technical aspects, technologies are not sufficient for all large point sources and also, largescale development should consider regarding the eco-friendliness. One of the major challenges associated with CCS is moving CO<sub>2</sub> storage to remote sites using CO<sub>2</sub> pipeline networks from the location it is captured to the storage site. These pipelines are costly, difficult to obtain permits and cause lot of environmental problems. As a suggestion, industries can be moved to remote storage sites.

There are several studies on the requirements and a working definition for carbon dioxide capture (CCS). Overall, it is required to develop some advanced physical adsorbents which have high CO<sub>2</sub> selectivity and gas uptake. Stability (over 1000 cycles), CO<sub>2</sub> affinity, scalability, reusability, resistance against surface erosion and additionally required energy are the major concerns in carbon capture. The sorbent cost is the most significant part of an air capture system; however, it is difficult to estimate the cost of a particular sorbent in lab scale experiments. According to the reported data, the value of a kilogram of sorbent is equal to the net present value of the CO<sub>2</sub> revenue collected during its lifetime. Therefore, it is necessary for a sorbent to possess constant stability and performance for its lifetime [181].

The other main challenges associated with sorbents are stability, kinetics, and sorbent capacity. However, thermodynamically, many sorbents are strong enough to capture CO<sub>2</sub> from ambient air and allowed for easy regeneration. Despite the reported data, further studies on stability, kinetics and capacity are still needed to be improved in SiO<sub>2</sub>-based adsorbents. Another factor is sorbent loading and unloading cycles since it is an important factor for reducing the cost. Also, kinetics is affected by binding energies and also by diffusion into porous materials and by the geometry of sorbent materials. According to the researchers, many sorbents require longer sorption times. Therefore, improved kinetics can lower the cost. High adsorption capacity can reduce the cost of CO<sub>2</sub> capture by reducing the amount of sorbent required. Physisorbents that selectively separate CO<sub>2</sub> from gaseous mixtures formed a revolution in CCS since it requires less energy for recycling, with enhanced CO<sub>2</sub> capacity. It is evident that a new generation of physisorbent materials is urgently required to address the carbon capture applications.

As a solution, amine-based sorbents are widely used during CCS. However, amine sorbent depends on the molecular weight of the sorbent and pore sizes of the sorbent. To improve the capacity of moisture-swing sorbents, the ion exchange resins can be prepared with a higher charge density, and materials with different of cation distances can be used under different humidity conditions. The potential of solid sorbents to remove CO<sub>2</sub> from flue gas is huge, compared to conventional liquid amine processes in terms of regeneration energy and significant cost reduction. However, as discussed previously, solid sorbents also have limitations and challenges to be addressed and solved before these can be deployed commercially in post-combustion CO<sub>2</sub> capture.

There is limited literature on CO<sub>2</sub> capture behavior of the silica-based materials synthesis using different low-cost silica sources such as rice husk. These sources lead to the reduction of production cost. Nevertheless, novel silica-based materials such as lithium orthosilicate (Li<sub>4</sub>SiO<sub>4</sub>), silica nano tubes, silica nano spheres, silica-based composites and silica aero gels lead to high CO<sub>2</sub> gas capture at elevated temperatures. Therefore, researchers should have focused on different silica-based materials for CO<sub>2</sub> capture.

Besides, currently, the majority of researchers have used sol gel, perception and hydrothermal process for synthesis of silica-based sorbent. However, apart from the aforementioned methods,

microwave treatment can be used which is a cost effective and time serving method. Moreover, different surfactants can be used for the preparation of silica with different pore sizes and morphologies. On the contrary, another issue raised with silica-based sorbent is the lack of literature on kinetic studies regarding the CO<sub>2</sub> adsorption and the removal of CO<sub>2</sub> from the natural gas sources at different temperatures. Moreover, silica-based sorbents need to be used with simulation work with the process design which might lead to successful deployment in industrial applications.

## 7. Conclusions

Here, a review on capture and the separation of CO<sub>2</sub> gas using different technologies is presented. Though chemical absorption is an energy intensive process, owing to the huge amount of relapsed CO<sub>2</sub> in power plants, chemical absorption is definitely more suitable than physical absorption to achieve a better CO<sub>2</sub> capture. Thus, due to the simplicity and lower regeneration energy requirements, sorption has been used a lot in the post-combustion CO<sub>2</sub> capture applications. This review paper is mainly focused on SiO<sub>2</sub>-based adsorbents used in this process. Apart from that, amine-functionalized SiO<sub>2</sub> possesses higher CO<sub>2</sub> selectivity over other gases and high CO<sub>2</sub> adsorption capacities which make them ideal candidates for CO<sub>2</sub> capture. Moreover, some of the experimental studies on these sorbents have been reported, compared and discussed. However, the performance of currently available amine functionalized SiO<sub>2</sub> should be further developed and improved in terms of stability, gas selectivity and resistivity to thermal degradation. Furthermore, the review pointed out some of the barriers and opportunities for CO<sub>2</sub> capture technology. More effective materials for CO<sub>2</sub> capture and storage are required to minimize the emissions of greenhouse gases.

**Author Contributions:** Conceptualization, S.M.A, C.A.G., Y.D., R.S.D, and E.C.; methodology, S.M.A, C.A.G.; software, S.M.A, O.H.P.G, C.A.G.; validation, S.M.A, C.A.G., Y.D., and R.S.D.; formal analysis, S.M.A, C.A.G.; investigation, S.M.A, C.A.G. Y.D., R.S.D, and E.C.; resources, S.M.A, C.A.G.; data curation, S.M.A, C.A.G.; writing—original draft preparation, S.M.A, O.H.P.G, C.A.G. and R.S.D.; writing—review and editing, S.M.A, C.A.G., Y.D., R.S.D, and E.C.; visualization, S.M.A, C.A.G., Y.D., and R.S.D; supervision, C.A.G. Y.D., R.S.D, and E.C.; project administration, C.A.G. Y.D., R.S.D, and E.C.; All authors have read and agreed to the published version of the manuscript.”.

**Funding:** E.-B. Cho acknowledges supports under the National Research Foundation of Korea (NRF-2022R111A2054213). .

**Acknowledgments:** The authors would like to express their gratitude to the Department of Chemical and Process Engineering, University of Peradeniya. This study was supported by the Human Resource Development Programs for Green Convergence Technology funded by the Korea Ministry of Environment (MOE).

**Conflicts of Interest:** The authors declare no conflict of interest.

## References

1. Osman, A.I.; Hefny, M.; Maksoud, M.A.; Elgarahy, A.M.; Rooney, D.W. Recent advances in carbon capture storage and utilisation technologies: a review. *Environ. Chem. Lett.* **2020**, 1-53.
2. Ahn, D. Quantifying the Emissions of Carbon Dioxide (CO<sub>2</sub>), Carbon Monoxide (Co), and Nitrogen Oxides (Nx) from Human Activities: Top-Down and Bottom-Up Approaches Doctoral dissertation, University of Maryland, College Park, USA, **2021**.
3. Gunawardene, O.H.; Gunathilake, C.A.; Vikrant, K.; Amaraweera, S.M. Carbon Dioxide Capture through Physical and Chemical Adsorption Using Porous Carbon Materials: A Review. *Atmosphere*. **2022**, 13(3), 397.
4. Leung, D.Y.; Caramanna, G.; Maroto-Valer, M.M. An overview of current status of carbon dioxide capture and storage technologies. *Renewable Sustainable Energy Rev.* **2014**, 39, 426-443.
5. Omoregbe, O.; Mustapha, A.N.; Steinberger-Wilckens, R.; El-Kharouf, A.; Onyeaka, H. Carbon capture technologies for climate change mitigation: A bibliometric analysis of the scientific discourse during 1998–2018. *Energy Reports*. **2020**, 6, 1200-1212.
6. Lee, S.Y.; Park, S.J.; A review on solid adsorbents for carbon dioxide capture. *J. Ind. Eng. Chem.* **2015**, 23, 1-11.
7. Bui, M.; Gunawan, I.; Verheyen, V.; Feron, P.; Meuleman, E.; Adeloju, S. Dynamic modelling and optimisation of flexible operation in post-combustion CO<sub>2</sub> capture plants—A review. *Comput. Chem. Eng.* **2014**, 61, 245-265.

8. Cotton, A.; Patchigolla, K.; Oakey, J.E.; Minor and trace element emissions from post-combustion CO<sub>2</sub> capture from coal: Experimental and equilibrium calculations. *Fuel*. **2014**. 117, 391-407.
9. Goto, K.; Yogo, K.; Higashii, T.; A review of efficiency penalty in a coal-fired power plant with post-combustion CO<sub>2</sub> capture. *Appl. Energy*. **2013**. 111, 710-720.
10. Zhang, N.; Pan, Z.; Zhang, Z.; Zhang, W.; Zhang, L.; Baena-Moreno, F.M.; Lichtfouse, E. CO<sub>2</sub> capture from coalbed methane using membranes: a review. *Environ. Chem. Lett.* **2020**. 18(1), 79-96.
11. Sreenivasalu, B.; Gayatri, D.V.; Sreedhar, I.; Ragharan, K.V. A journey into the process and engineering aspects of carbon capture technologies. *Renew. Sustain. Energy Rev.* **2015**, 41, 1324–1350
12. Singh, J.; Bhunia, H.; Basu, S.; Development of sulfur-doped carbon monolith derived from phenol-formaldehyde resin for fixed bed CO<sub>2</sub> adsorption. *Environmental and Innovation*. **2020**. 20, 101104.
13. Sánchez, J.M.; Maroño, M.; Cillero, D.; Montenegro, L.; Ruiz, E.; Laboratory-and bench-scale studies of a sweet water-gas-shift catalyst for H<sub>2</sub> and CO<sub>2</sub> production in pre-combustion CO<sub>2</sub> capture. *Fuel*. **2013**. 114, 191-198.
14. Babu, P.; Kumar, R.; Linga, P. A new porous material to enhance the kinetics of clathrate process: application to precombustion carbon dioxide capture. *Environ. Sci. Technol.* **2013**. 47(22), 13191-13198.
15. Wienchol P.; Szlęk A.; Ditaranto M.; Waste-to-energy technology integrated with carbon capture—challenges and opportunities. *Energy*. **2020**. 198:117352. ISSN 0360-5442.
16. Kim, Y.E.; Moon, S.J.; Yoon, Y.I.; Jeong, S.K.; Park, K.T.; Bae, S.T.; Nam, S.C.; Heat of absorption and absorption capacity of CO<sub>2</sub> in aqueous solutions of amine containing multiple amino groups. *Separation and Purification Technology*. **2014**. 122, 112-118.
17. Roth, E.A.; Agarwal, S.; Gupta, R.K.; Nanoclay-based solid sorbents for CO<sub>2</sub> capture. *Energy and fuels*. **2013**. 27(8), 4129-4136.
18. Kenarsari, S.D.; Yang, D.; Jiang, G.; Zhang, S.; Wang, J.; Russell, A.G.; Wei, Q.; Fan, M. Review of recent advances in carbon dioxide separation and capture. *Rsc Advances*. **2013**. 3(45), 22739-22773.
19. Zhang, X.; He, X.; Gundersen, T. Post-combustion carbon capture with a gas separation membrane: parametric study, capture cost, and exergy analysis. *Energy and Fuels*. **2013**. 27(8), 4137-4149.
20. Scholes, C.A.; Ho, M.T.; Wiley, D.E.; Stevens, G.W.; Kentish, S.E. Cost competitive membrane—cryogenic post-combustion carbon capture. *Int. J. Greenh. Gas Control.*, **2013**. 17, 341-348.
21. Khraisheh, M.; Mukherjee, S.; Kumar, A.; Al Momani, F.; Walker, G.; Zaworotko, M.J.; An overview on trace CO<sub>2</sub> removal by advanced physisorbent materials. *Journal of environmental management*. **2020**. 255, 109874.
22. Anwar, M.N.; Fayyaz, A.; Sohail, N.F.; Khokhar, M.F.; Baqar, M.; Khan, W.D.; Rasool, K.; Rehan, M.; Nizami, A.S. CO<sub>2</sub> capture and storage: a way forward for sustainable environment. *Journal of environmental management*. **2018**. 226, 131-144.
23. Xu, G.; Liang, F.; Yang, Y.; Hu, Y.; Zhang, K.; Liu, W. An improved CO<sub>2</sub> separation and purification system based on cryogenic separation and distillation theory. *Energies*. **2014**. 7(5), 3484-3502.
24. Samanta, A.; Zhao, A.; Shimizu, G.K.; Sarkar, P.; Gupta, R. Post-combustion CO<sub>2</sub> capture using solid sorbents: a review. *Ind. Eng. Chem. Res.* **2012**. 51(4), 1438-1463.
25. Patel, H.A.; Byun, J.; Yavuz, C.T. Carbon dioxide capture adsorbents: chemistry and methods. *Chem. Sus. Chem.*, **2017**. 10(7), 1303-1317.
26. Sumida, K.; Rogow, D.L.; Mason, J.A.; McDonald, T.M.; Bloch, E.D.; Herm, Z.R.; Bae, T.H.; Long, J.R. Carbon dioxide capture in metal-organic frameworks. *Chemical reviews*. **2012**. 112(2), 724-781.
27. Reynolds, A.J.; Verheyen, T.V.; Adeloju, S.B.; Meuleman, E.; Feron, P. Towards commercial scale postcombustion capture of CO<sub>2</sub> with monoethanolamine solvent: key considerations for solvent management and environmental impacts. *Environ. Sci. Technol.* **2012**. 46(7), 3643-3654.
28. Mumford, K.A.; Wu, Y.; Smith, K.H.; Stevens, G.W. Review of solvent based carbon-dioxide capture technologies. *Front Chem Sci Eng.* **2015**. 9(2), 125-141.
29. Park, J.H.; Celedonio, J.M.; Seo, H.; Park, Y.K. Ko, Y.S. A study on the effect of the amine structure in CO<sub>2</sub> dry sorbents on CO<sub>2</sub> capture. *Catalysis Today*. **2016**. 265, 68-76.
30. Gunathilake, C.; Gangoda, M.; Jaroniec, M. Mesoporous alumina with amidoxime groups for CO<sub>2</sub> sorption at ambient and elevated temperatures. *Ind. Eng. Chem. Res.* **2016**. 55(19), 5598-5607.
31. Lv, B.; Guo, B.; Zhou, Z.; Jing, G. Mechanisms of CO<sub>2</sub> capture into monoethanolamine solution with different CO<sub>2</sub> loading during the absorption/desorption processes. *Environ. Sci. Technol.* **2015**. 49(17), 10728-10735.
32. García-Abuín, A.; Gomez-Diaz, D.; Lopez, A.B.; Navaza, J.M.; Rumbo, A. NMR characterization of carbon dioxide chemical absorption with monoethanolamine, diethanolamine, and triethanolamine. *Ind. Eng. Chem. Res.* **2013**. 52(37), 13432-13438.



33. Kim, Y.E.; Lim, J.A.; Jeong, S.K.; Yoon, Y.I.; Bae, S.T.; Nam, S.C. Comparison of carbon dioxide absorption in aqueous MEA, DEA, TEA, and AMP solutions. *Bulletin of the Korean Chemical Society*. **2013**. 34(3), 783-787.
34. Rinprasertmeechai, S.; Chavadej, S.; Rangsunvigit, P.; Kulprathipanja, S. Carbon dioxide removal from flue gas using amine-based hybrid solvent absorption. *Int. J. Chem. Eng.* **2012**. 6, 296-300.
35. Aaron, D.; Tsouris, C. Separation of CO<sub>2</sub> from flue gas: a review. *Sep Sci Technol.* **2005**. 40(1-3), 321-348.
36. Songolzadeh, M.; Soleimani, M.; Takht Ravanchi, M.; Songolzadeh, R. Carbon dioxide separation from flue gases: a technological review emphasizing reduction in greenhouse gas emissions. *The Scientific World Journal*. **2014**. 2014.
37. Wang, M.; Lawal, A.; Stephenson, P.; Sidders, J.; Ramshaw, C. Post-combustion CO<sub>2</sub> capture with chemical absorption: A state-of-the-art review. *Chem Eng Res Des.* **2011**. 89(9), 1609-1624.
38. Dave, N.; Do, T.; Puxty, G.; Rowland, R.; Feron, P.H.M.; Attalla, M.I. CO<sub>2</sub> capture by aqueous amines and aqueous ammonia—A Comparison. *Energy Procedia*. **2009**. 1(1), 949-954.
39. Zeng, S.; Zhang, X.; Bai, L.; Zhang, X.; Wang, H.; Wang, J.; Bao, D.; Li, M.; Liu, X.; Zhang, S. Ionic-liquid-based CO<sub>2</sub> capture systems: structure, interaction and process. *Chemical reviews*. **2017**. 117(14), 9625-9673.
40. Borhani, T.N.; Wang, M. Role of solvents in CO<sub>2</sub> capture processes: The review of selection and design methods. *Renewable Sustainable Energy Rev.* **2019**. 114, 109299.
41. Aghaie, M.; Rezaei, N.; Zendehboudi, S. A systematic review on CO<sub>2</sub> capture with ionic liquids: Current status and future prospects. *Renewable Sustainable Energy Rev.* **2018**. 96, 502-525.
42. Jin, X.; Ge, J.; Zhang, L.; Wu, Z.; Zhu, L.; Xiong, M. Synthesis of Hierarchically Ordered Porous Silica Materials for CO<sub>2</sub> Capture: The Role of Pore Structure and Functionalized Amine. *Inorganics*. **2022**. 10(7), 87.
43. Zagho, M.M.; Hassan, M.K.; Khraisheh, M.; Al-Maadeed, M.A.A.; Nazarenko, S. A review on recent advances in CO<sub>2</sub> separation using zeolite and zeolite-like materials as adsorbents and fillers in mixed matrix membranes (MMMs). *Chemical Engineering Journal Advances*. **2021**. 6, 100091.
44. Yu, C.H.; Huang, C.H.; Tan, C.S. A review of CO<sub>2</sub> capture by absorption and adsorption. *Aerosol and Air Quality Research*. **2012**. 12(5), 745-769.
45. Kumar, S.; Bera, R.; Das, N.; Koh, J. Chitosan-based Zeolite-Y and ZSM-5 porous biocomposites for H<sub>2</sub> and CO<sub>2</sub> storage. *Carbohydr. Polym.* **2020**. 232, 115808.
46. Kumar, S.; Srivastava, R.; Koh, J. Utilization of zeolites as CO<sub>2</sub> capturing agents: Advances and future perspectives. *J. CO<sub>2</sub> Util.* **2020**. 41, 101251.
47. Balashankar, V.S.; Rajendran, A. Process optimization-based screening of zeolites for post-combustion CO<sub>2</sub> capture by vacuum swing adsorption. *ACS Sustain. Chem. Eng.* **2019**. 7(21), 17747-17755.
48. Avci, G.; Erucar, I.; Keskin, S. Do new MOFs perform better for CO<sub>2</sub> capture and H<sub>2</sub> purification? Computational screening of the updated MOF database. *ACS Applied Materials & Interfaces*. **2020**. 12(37), 41567-41579.
49. Modak, A.; Jana, S. Advancement in porous adsorbents for post-combustion CO<sub>2</sub> capture. *Microporous Mesoporous Mater.* **2019**. 276, 107-132.
50. Le, M.U.T.; Lee, S.Y.; Park, S.J. Preparation and characterization of PEI-loaded MCM-41 for CO<sub>2</sub> capture. *Int. J. Hydrog. Energy*. **2014**. 39(23), 12340-12346.
51. Kim, M.I.; Choi, S.J.; Kim, D.W.; Park, D.W. Catalytic performance of zinc containing ionic liquids immobilized on silica for the synthesis of cyclic carbonates. *J Ind Eng Chem.* **2014**. 20(5), 3102-3107.
52. Alkhabbaz, M.A.; Khunsupat, R.; Jones, C.W. Guanidinylated poly (allylamine) supported on mesoporous silica for CO<sub>2</sub> capture from flue gas. *Fuel*. **2014**. 121, 79-85.
53. Reddy, M.S.B.; Ponnammma, D.; Sadasivuni, K.K.; Kumar, B.; Abdullah, A.M. Carbon dioxide adsorption based on porous materials. *RSC Advances*. **2021**. 11(21), 12658-12681.
54. Liu, R.S.; Shi, X.D.; Wang, C.T.; Gao, Y.Z.; Xu, S.; Hao, G.P.; Chen, S.; Lu, A.H. Advances in Post-Combustion CO<sub>2</sub> Capture by Physical Adsorption: From Materials Innovation to Separation Practice. *Chem Sus Chem*. **2021**. 14(6), 1428-1471.
55. Boot-Handford, M.E.; Abanades, J.C.; Anthony, E.J.; Blunt, M.J.; Brandani, S.; Mac Dowell, N.; Fernández, J.R.; Ferrari, M.C.; Gross, R.; Hallett, J.P.; Haszeldine, R.S. Carbon capture and storage update. *Energy Environ. Sci.* **2014**. 7(1), 130-189.
56. MacFarlane, D.R.; Tachikawa, N.; Forsyth, M.; Pringle, J.M.; Howlett, P.C.; Elliott, G.D.; Davis, J.H.; Watanabe, M.; Simon, P.; Angell, C.A. Energy applications of ionic liquids. *Energy Environ. Sci.* **2014**. 7(1), 232-250.
57. Patel, H.A.; Byun, J.; Yavez, C.T. Carbon dioxide capture adsorbents: Chemistry and Methods. *Chem Sus Chem* **2017**, 10, 1303–1317.

58. Tuci, G.; Iemhoff, A.; Ba, H.; Luconi, L.; Rossin, A.; Papaefthimiou, V.; Palkovits, R.; Artz, J.; Pham-Huu, C.; Giambastiani, G. Playing with covalent triazine framework tiles for improved CO<sub>2</sub> adsorption properties and catalytic performance. *Beilstein journal of nanotechnology*. **2019**. 10(1), 1217-1227.
59. Madden, D.G.; O’Nolan, D.; Chen, K.J.; Hua, C.; Kumar, A.; Pham, T.; Forrest, K.A.; Space, B.; Perry, J.J.; Khraisheh, M.; Zaworotko, M.J. Highly selective CO<sub>2</sub> removal for one-step liquefied natural gas processing by physisorbents. *Chemical Communications*. **2019**, 55(22), 3219-3222.
60. Balsamo, M.; Budinova, T.; Erto, A.; Lancia, A.; Petrova, B.; Petrov, N.; Tsyntsarski, B. CO<sub>2</sub> adsorption onto synthetic activated carbon: Kinetic, thermodynamic and regeneration studies. *Separation and purification technology*. **2013**. 116, 214-221.
61. Sreenivasalu, B.; Gayatri, D.V.; Sreedhar, I.; Ragharan, K.V. A journey into the process and engineering aspects of carbon capture technologies. *Renew. Sustain. Energy Rev.* **2015**, 41, 1324–1350.
62. Cherbanski, R.; Komorowska-Durka, M.; Stefanidis, G.D.; Stankiewicz, A.I. Microwave Swing Regeneration Vs Temperature Swing Regeneration Comparison of Desorption Kinetics. *Ind. Eng. Chem. Res.* **2011**. 50(14), 8632-8644.
63. Maity, A.; Belgamwar, R.; Polshettiwar, V. Facile synthesis to tune size, textural properties and fiber density of dendritic fibrous nanosilica for applications in catalysis and CO<sub>2</sub> capture. *Nature protocols*. **2019**. 14(7), 2177-2204.
64. Miricioiu, M.G.; Niculescu, V.C. Fly ash, from recycling to potential raw material for mesoporous silica synthesis. *Nanomaterials*. **2020**. 10(3), 474.
65. Wan, Ying, Dongyuan Zhao. On the controllable soft-templating approach to mesoporous silicates. *Chemical reviews*. **2007**. 107, no. 7 (2007): 2821-2860.
66. Narayan, R.; Nayak, U.Y.; Raichur, A.M.; Garg, S. Mesoporous silica nanoparticles: A comprehensive review on synthesis and recent advances. *Pharmaceutics*. **2018**. 10(3), 118.
67. Costa, J.A.S.; de Jesus, R.A.; Santos, D.O.; Mano, J.F.; Romao, L.P.; Paranhos, C.M. Recent progresses in the adsorption of organic, inorganic, and gas compounds by MCM-41-based mesoporous materials. *Microporous and Mesoporous Materials*, **2020**. 291, 109698.
68. Brezoiu, A.M.; Deaconu, M.; Nicu, I.; Vasile, E.; Mitran, R.A.; Matei, C.; Berger, D. Heteroatom modified MCM-41-silica carriers for Lomefloxacin delivery systems. *Microporous and Mesoporous Materials*, **2019**. 275, 214-222.
69. Jesus, R.A.; Rabelo, A.S.; Figueiredo, R.T.; Da Silva, L.C.; Codentino, I.C.; Fantini, M.C.D.A.; Araújo, G.L.B.D.; Araújo, A.A.S.; Mesquita, M.E. Synthesis and application of the MCM-41 and SBA-15 as matrices for in vitro efavirenz release study. *J Drug Deliv Sci Technol*. **2016**, 31, 153-159.
70. Liu, Y.; Li, C.; Peyravi, A.; Sun, Z.; Zhang, G.; Rahmani, K.; Zheng, S.; Hashisho, Z. Mesoporous MCM-41 derived from natural Opoka and its application for organic vapors removal. *J. Hazard. Mater.* **2021**. 408, 124911.
71. Costa, J.A.S.; Paranhos, C.M. Mitigation of silica-rich wastes: an alternative to the synthesis eco-friendly silica-based mesoporous materials. *Microporous and Mesoporous Materials*, **2020**. 309, 110570.
72. Björk, E.M. Synthesizing and characterizing mesoporous silica SBA-15: A hands-on laboratory experiment for undergraduates using various instrumental techniques. *J. Chem. Educ.*, **2017**. 94(1), 91-94.
73. Martínez, M.L.; Ponte, M.V.; Beltramone, A.R.; Anunziata, O.A. Synthesis of ordered mesoporous SBA-3 materials using silica gel as silica source. *Materials Letters*, **2014**. 134, 95-98.
74. López-Mendoza, M.A.; Nava, R.; Peza-Ledesma, C.; Millán-Malo, B.; Huirache-Acuña, R.; Skewes, P.; Rivera-Muñoz, E.M. Characterization and catalytic performance of Co-Mo-W sulfide catalysts supported on SBA-15 and SBA-16 mechanically mixed. *Catalysis Today*, **2016**. 271, 114-126.
75. Gonzalez, G.; Sagarzazu, A.; Cordova, A.; Gomes, M.E.; Salas, J.; Contreras, L.; Noris-Suarez, K.; Lascano, L. Comparative study of two silica mesoporous materials (SBA-16 and SBA-15) modified with a hydroxyapatite layer for clindamycin controlled delivery. *Microporous and Mesoporous Materials*, **2018**. 256, 251-265.
76. Wu, Q.; Li, Y.; Hou, Z.; Xin, J.; Meng, Q.; Han, L.; Xiao, C.; Hu, D.; Duan, A.; Xu, C. Synthesis and characterization of Beta-FDU-12 and the hydrosulfurization performance of FCC gasoline and diesel. *Fuel processing technology*, **2018**. 172, 55-64.
77. Sanaeishoar, H.; Sabbaghan, M.; Mohave, F.; Nazarpour, R. Disordered mesoporous KIT-1 synthesized by DABCO-based ionic liquid and its characterization. *Microporous and Mesoporous Materials*, **2016**. 228, 305-309.
78. Stöber W.; Fink A.; Bohn E. Controlled growth of monodisperse silica spheres in micron size range. *J. Colloid Interface Sci*, **1968**. 26, 62-69.



79. Choma, J.; Jamiola, D.; Augustynek, K.; Marszewski, M.; Gao, M.; Jaroniec, M. New opportunities in Stober synthesis: preparation of microporous and mesoporous carbon spheres. *J. Mater. Chem.* **2012**, 22(25), 12636-12642.
80. Wu, S.H.; Mou, C.Y.; Lin, H.P. Synthesis of mesoporous silica nanoparticles. *Chem Soc Rev.* **2013**, 42(9), 3862-3875.
81. Sakamoto, S.; Yoshikawa, M.; Ozawa, K.; Kuroda, Y.; Shimojima, A.; Kuroda, K. Formation of single-digit nanometer scale silica nanoparticles by evaporation-induced self-assembly. *Langmuir.* **2018**, 34(4), 1711-1717.
82. Sihler, S.; Nguyen, P.L.; Lindén, M.; Ziener, U. Green chemistry in red emulsion: Interface of dye stabilized emulsions as a powerful platform for the formation of sub-20-nm SiO<sub>2</sub> nanoparticles. *ACS Appl. Mater. Interfaces.* **2018**, 10(28), 24310-24319.
83. Murray, E.; Born, P.; Weber, A.; Kraus, T. Synthesis of Monodisperse Silica Nanoparticles Dispersable in Non-Polar Solvents. *Adv. Eng. Mater.* **2010**, 12(5), 374-378.
84. Mandal, M.; Kruk, M. Family of single-micelle-templated organosilica hollow nanospheres and nanotubes synthesized through adjustment of organosilica/surfactant ratio. *Chem. Mater.* **2012**, 24(1), 123-132.
85. Savic, S.; Vojisavljevic, K.; Počuča-Nešić, M.; Zivojevic, K.; Mladenovic, M.; Knezevic, N. Hard Template Synthesis of Nanomaterials Based on Mesoporous Silica. *Metall. Mater. Eng.* **2018**, 24(4).
86. Zhao, T.; Elzatahry, A.; Li, X.; Zhao, D. Single-micelle-directed synthesis of mesoporous materials. *Nat. Rev. Mater.* **2019**, 4(12), 775-791.
87. Khan, A.H.; Ghosh, S.; Pradhan, B.; Dalui, A.; Shrestha, L.K.; Acharya, S.; Ariga, K. Two-dimensional (2D) nanomaterials towards electrochemical nanoarchitectonics in energy-related applications. *Bulletin of the Chemical Society of Japan.* **2017**, 90(6), 627-648.
88. Yamamoto, E.; Kuroda, K. Colloidal mesoporous silica nanoparticles. *Bulletin of the chemical society of Japan.* **2016**, 89(5), 501-539.
89. Kim, H.J.; Yang, H.C.; Chung, D.Y.; Yang, I.H.; Choi, Y.J.; Moon, J.K. Functionalized mesoporous silica membranes for CO<sub>2</sub> separation applications. *J. Chem.* **2015**, 2015.
90. Gunathilake, C.; Kalpage, C.; Kadanapitiye, M.; Dassanayake, R.S.; Manchanda, A.S.; Gangoda, M. Facile synthesis and surface characterization of titania-incorporated mesoporous organosilica materials. *J. Compos. Sci.* **2019**, 3(3), 77.
91. Hao, P.; Peng, B.; Shan, B.Q.; Yang, T.Q.; Zhang, K. Comprehensive understanding of the synthesis and formation mechanism of dendritic mesoporous silica nanospheres. *Nanoscale Adv.* **2020**, 2(5), 1792-1810.
92. Panek, R.; Wdowin, M.; Franus, W.; Czarna, D.; Stevens, L.A.; Deng, H.; Liu, J.; Sun, C.; Liu, H.; Snape, C.E. Fly ash-derived MCM-41 as a low-cost silica support for polyethyleneimine in post-combustion CO<sub>2</sub> capture. *J. CO<sub>2</sub> Util.* **2017**, 22, 81-90.
93. Singh, B.; Polshettiwar, V. Solution-phase synthesis of two-dimensional silica nanosheets using soft templates and their applications in CO<sub>2</sub> capture. *Nanoscale*, **2019**, 11(12), 5365-5376.
94. Li, Y.; Wang, X.; Cao, M. Three-dimensional porous carbon frameworks derived from mangosteen peel waste as promising materials for CO<sub>2</sub> capture and supercapacitors. *J. CO<sub>2</sub> Util.* **2018**, 27, 204-216.
95. Ahmed, S.; Ramli, A.; Yusup, S. Development of polyethylenimine-functionalized mesoporous Si-MCM-41 for CO<sub>2</sub> adsorption. *Fuel Processing Technology*, **2017**, 167, 622-630.
96. Son, W.J.; Choi, J.S.; Ahn, W.S. Adsorptive removal of carbon dioxide using polyethyleneimine-loaded mesoporous silica materials. *Microporous and Mesoporous Materials*. **2008**, 113(1-3), 31-40.
97. Zelenák, V.; Badaničová, M.; Halamová, D.; Čejka, J.; Zúkal, A.; Murafo, N.; Goerigk, G. Amine-modified ordered mesoporous silica: effect of pore size on carbon dioxide capture. *Chemical Engineering Journal*, **2008**, 144(2), 336-342.
98. Lashaki, M.J.; Sayari, A. CO<sub>2</sub> capture using triamine-grafted SBA-15: The impact of the support pore structure. *Chemical Engineering Journal*, **2018**, 334, 1260-1269.
99. Kishor, R.; Ghoshal, A.K. APTES grafted ordered mesoporous silica KIT-6 for CO<sub>2</sub> adsorption. *Chemical Engineering Journal*, **2015**, 262, 882-890.
100. Ahmed, S.; Ramli, A.; Yusup, S. CO<sub>2</sub> adsorption study on primary, secondary and tertiary amine functionalized Si-MCM-41. *Int. J. Greenh. Gas Control*. **2016**, 51, 230-238.
101. Nigar, H.; Garcia-Baños, B.; Peñaranda-Foix, F.L.; Catalá-Civera, J.M.; Mallada, R.; Santamaría, J. Amine-functionalized mesoporous silica: A material capable of CO<sub>2</sub> adsorption and fast regeneration by microwave heating. *AIChE Journal*. **2016**, 62(2), 547-555.
102. Heydari-Gorji, A.; Yang, Y.; Sayari, A. Effect of the pore length on CO<sub>2</sub> adsorption over amine-modified mesoporous silicas. *Energy and Fuels*. **2011**, 25(9), 4206-4210.
103. Gunathilake, C.; Manchanda, A.S.; Ghimire, P.; Kruk, M.; Jaroniec, M. Amine-modified silica nanotubes and nanospheres: synthesis and CO<sub>2</sub> sorption properties. *Environ. Sci.* **2016**, 3(4), 806-817.

104. Cabriga, C.K.C.; Clarete, K.V.R.; Zhang, J.A.T.; Pacia, R.M.P.; Ko, Y.S.; Castro, J.C. Evaluation of biochar derived from the slow pyrolysis of rice straw as a potential adsorbent for carbon dioxide. *Biomass Convers. Biorefinery* **2021**.
105. Wang, J.; Yuan, X.; Deng, S.; Zeng, X.; Yu, Z.; Li, S.; Lia, K. Waste polyethylene terephthalate (PET) plastics-derived activated carbon for CO<sub>2</sub> capture: A route to a closed carbon loop. *Green Chem.* **2020**, *22*, 6836–6845.
106. Berger, A.H.; Bhowan, A.S. Comparing physisorption and chemisorption solid sorbents for use separating CO<sub>2</sub> from flue gas using temperature swing adsorption. *Energy Proc.* **2011**, *4*, 562–567.
107. Moni, P.; Chaves, W.F.; Wilhelm, M.; Rezwan, K. Polysiloxane microspheres encapsulated in carbon allotropes: A promising material for supercapacitor and carbon dioxide capture. *Journal of colloid and interface science*, **2019**, *542*, 91–101.
108. Hahn, M.W.; Jelic, J.; Berger, E.; Reuter, K.; Jentys, A.; Lercher, J.A. Role of amine functionality for CO<sub>2</sub> chemisorption on silica. *The Journal of Physical Chemistry B*, **2016**, *120*(8), 1988–1995.
109. Chen, C.; Yang, S.T.; Ahn, W.S.; Ryoo, R. Amine-impregnated silica monolith with a hierarchical pore structure: enhancement of CO<sub>2</sub> capture capacity. *Chemical Communications*, **2009**, (24), 627–3629.
110. Chen, C.; Son, W.J.; You, K.S.; Ahn, J.W.; Ahn, W.S. Carbon dioxide capture using amine-impregnated HMS having textural mesoporosity. *Chemical Engineering Journal*, **2010**, *161*(1-2), 46–52.
111. Chen, C.; Zhang, S.; Row, K.H.; Ahn, W.S. Amine–silica composites for CO<sub>2</sub> capture: A short review. *Journal of energy chemistry*, **2017**, *26*(5), 868–880.
112. Wei, J.; Liao, L.; Xiao, Y.; Zhang, P.; Shi, Y. Capture of carbon dioxide by amine-impregnated as-synthesized MCM-41. *Journal of Environmental Sciences*, **2010**, *22*(10), 1558–1563.
113. Chew, T.L.; Ahmad, A.L.; Bhatia, S. Ordered mesoporous silica (OMS) as an adsorbent and membrane for separation of carbon dioxide (CO<sub>2</sub>). *Adv. Colloid Interface Sci.* **2010**, *153*(1-2), 43–57.
114. Li, W.; Choi, S.; Drese, J.H.; Hornbostel, M.; Krishnan, G.; Eisenberger, P.M.; Jones, C.W. Steam-stripping for regeneration of supported amine-based CO<sub>2</sub> adsorbents. *Chem Sus Chem*, **2010**, *3*(8), 899–903.
115. Bollini, P.; Didas, S.A.; Jones, C.W. Amine-oxide hybrid materials for acid gas separations. *J. Mater. Chem.* **2011**, *21*(39), 15100–15120.
116. Li, Y.; Sun, N.; Li, L.; Zhao, N.; Xiao, F.; Wei, W.; Sun, Y.; Huang, W. Grafting of amines on ethanol-extracted SBA-15 for CO<sub>2</sub> adsorption. *Materials*, **2013**, *6*(3), 981–999.
117. Lopez-Aranguren, P.; Builes, S.; Fraile, J.; Vega, L.F.; Domingo, C. Understanding the performance of new amine-functionalized mesoporous silica materials for CO<sub>2</sub> adsorption. *Ind. Eng. Chem. Res.* **2014**, *53*(40), 15611–15619.
118. Sanz, R.; Calleja, G.; Arencibia, A.; Sanz-Perez, E.S. CO<sub>2</sub> capture with pore-expanded MCM-41 silica modified with amino groups by double functionalization. *Microporous and Mesoporous Materials*. **2015**. 209, 165–171.
119. Wang, X.; Guo, Q.; Zhao, J.; Chen, L. Mixed amine-modified MCM-41 sorbents for CO<sub>2</sub> capture. *Int. J. Greenh. Gas Control*. **2015**, *37*, 90–98.
120. Jung, H.; Lee, C.H.; Jeon, S.; Jo, D.H.; Huh, J.; Kim, S.H. Effect of amine double-functionalization on CO<sub>2</sub> adsorption behaviors of silica gel-supported adsorbents. *Adsorption*. **2016**, *22*(8), 1137–1146.
121. Fillerup, E.; Zhang, Z.; Peduzzi, E.; Wang, D.; Guo, J.; Ma, X.; Wang, X.; Song, C. CO Capture from Flue Gas Using Solid Molecular Basket Sorbents. The Pennsylvania State University. **2012**.
122. Gargiulo, N.; Peluso, A.; Aprea, P.; Pepe, F.; Caputo, D. CO<sub>2</sub> adsorption on polyethylenimine-functionalized SBA-15 mesoporous silica: isotherms and modeling. *J. Chem. Eng. Data*. **2014**. *59*(3), 896–902.
123. Heydari-Gorji, A.; Sayari, A.; Thermal, oxidative, and CO<sub>2</sub>-induced degradation of supported polyethylenimine adsorbents. *Ind. Eng. Chem. Res.*, **2012**. *51*(19), 6887–6894.
124. Kuwahara, Y.; Kang, D.Y.; Copeland, J.R.; Brunelli, N.A.; Didas, S.A.; Bollini, P.; Sievers, C.; Kamegawa, T.; Yamashita, H.; Jones, C.W. Dramatic enhancement of CO<sub>2</sub> uptake by poly (ethyleneimine) using zirconsilicate supports. *J. Am. Chem. Soc.* **2012**. *134*(26), 10757–10760.
125. Kishor, R.; Ghoshal, A.K. Amine-modified mesoporous silica for CO<sub>2</sub> adsorption: the role of structural parameters. *Ind. Eng. Chem. Res.*, **2017**. *56*(20), 6078–6087.
126. Ko, Y.G.; Lee, H.J.; Oh, H.C.; Choi, U.S. Amines immobilized double-walled silica nanotubes for CO<sub>2</sub> capture. *J. Hazard. Mater.* **2013**. *250*, 53–60.
127. Choi, S.; Drese, J.H.; Eisenberger, P.M.; Jones, C.W. Application of amine-tethered solid sorbents for direct CO<sub>2</sub> capture from the ambient air. *Environ. Sci. Technol.* **2011**. *45*(6), 2420–2427.
128. Guo, X.; Ding, L.; Kanamori, K.; Nakanishi, K.; Yang, H. Functionalization of hierarchically porous silica monoliths with polyethyleneimine (PEI) for CO<sub>2</sub> adsorption. *Microporous and Mesoporous Materials*, **2017**. *245*, 51–57.
129. Liu, Z.; Teng, Y.; Zhang, K.; Chen, H.; Yang, Y. CO<sub>2</sub> adsorption performance of different amine-based siliceous MCM-41 materials. *J. Energy Chem.* **2015**. *24*(3), 322–330.

130. de Carvalho, L.S.; Silva, E.; Andrade, J.C.; Silva, J.A.; Urbina, M.; Nascimento, P.F.; Carvalho, F.; Ruiz, J.A. 2015. Low-cost mesoporous adsorbents amines-impregnated for CO<sub>2</sub> capture. *Adsorption*. **2015**, 21(8), 597-609.
131. López-Aranguren, P.; Builes, S.; Fraile, J.; López-Periago, A.; Vega, L.F.; Domingo, C. Hybrid aminopolymer-silica materials for efficient CO<sub>2</sub> adsorption. *RSC advances*. **2015**, 5(127), 104943-104953.
132. Mello, M.R.; Phanon, D.; Silveira, G.Q.; Llewellyn, P.L.; Ronconi, C.M. Amine-modified MCM-41 mesoporous silica for carbon dioxide capture. *Microporous and Mesoporous Materials*. **2011**, 143(1), 174-179.
133. Ahmed, S.; Ramli, A.; Yusup, S.; Farooq, M. Adsorption behavior of tetraethylenepentamine-functionalized Si-MCM-41 for CO<sub>2</sub> adsorption. *Chem Eng Res Des*. **2017**, 122, 33-42.
134. Niu, M.; Yang, H.; Zhang, X.; Wang, Y.; Tang, A. Amine-impregnated mesoporous silica nanotube as an emerging nanocomposite for CO<sub>2</sub> capture. *ACS Appl. Mater. Interfaces*. **2016**, 8(27), 17312-17320.
135. Ullah, R.; Atilhan, M.; Aparicio, S.; Canlier, A.; Yavuz, C.T. 2015. Insights of CO<sub>2</sub> adsorption performance of amine impregnated mesoporous silica (SBA-15) at wide range pressure and temperature conditions. *Int. J. Greenh. Gas Control*. **2015**, 43, 22-32.
136. Sánchez-Vicente, Y.; Stevens, L.A.; Pando, C.; Torralvo, M.J.; Snape, C.E.; Drage, T.C.; Cabañas, A. 2015. A new sustainable route in supercritical CO<sub>2</sub> to functionalize silica SBA-15 with 3-aminopropyltrimethoxysilane as material for carbon capture. *J. Chem. Eng.* **2015**, 264, 886-898.
137. Zhao, A.; Samanta, A.; Sarkar, P.; Gupta, R. 2013. Carbon dioxide adsorption on amine-impregnated mesoporous SBA-15 sorbents: experimental and kinetics study. *Ind. Eng. Chem. Res.* **2013**, 52(19), 6480-6491.
138. Gholami, M.; Talaie, M.R.; Aghamiri, S.F. Direct synthesis of bi-modal porous structure MCM-41 and its application in CO<sub>2</sub> capturing through amine-grafting. *Korean Journal of Chemical Engineering*. **2014**, 31(2), 322-326.
139. Loganathan, S.; Tikmani, M.; Ghoshal, A.K. Novel pore-expanded MCM-41 for CO<sub>2</sub> capture: synthesis and characterization. *Langmuir*. **2013**, 29(10), 3491-3499.
140. Kassab, H.; Maksoud, M.; Aguado, S.; Pera-Titus, M.; Albela, B. Bonneviot, L. Polyethylenimine covalently grafted on mesostructured porous silica for CO<sub>2</sub> capture. *RSC advances*. **2012**, 2(6), 2508-2516.
141. Teng, Y.; Li, L.; Xu, G.; Zhang, K.; Li, K. Promoting effect of inorganic alkali on carbon dioxide adsorption in amine-modified MCM-41. *Energies*. **2016**, 9(9), 667.
142. Sharma, P.; Seong, J.K.; Jung, Y.H.; Choi, S.H.; Park, S.D.; Yoon, Y.I. Baek, I.H. Amine modified and pelletized mesoporous materials: Synthesis, textural-mechanical characterization and application in adsorptive separation of carbondioxide. *Powder technology*. **2012**, 219, 86-98.
143. Yan, X.; Komarneni, S.; Yan, Z. CO<sub>2</sub> adsorption on Santa Barbara Amorphous-15 (SBA-15) and amine-modified Santa Barbara Amorphous-15 (SBA-15) with and without controlled microporosity. *J. Colloid Interface Sci.* **2013**, 390(1), 217-224.
144. Sanz, R.; Calleja, G.; Arencibia, A.; Sanz-Pérez, E.S. Amino functionalized mesostructured SBA-15 silica for CO<sub>2</sub> capture: Exploring the relation between the adsorption capacity and the distribution of amino groups by TEM. *Microporous and Mesoporous Materials*. **2012**, 158, 309-317.
145. Rao, N.; Wang, M.; Shang, Z.; Hou, Y.; Fan, G.; Li, J. CO<sub>2</sub> adsorption by amine-functionalized MCM-41: a comparison between impregnation and grafting modification methods. *Energy and Fuels*. **2018**, 32(1), 670-677.
146. Sim, K.; Lee, N.; Kim, J.; Cho, E.B.; Gunathilake, C.; Jaroniec, M. CO<sub>2</sub> adsorption on amine-functionalized periodic mesoporous benzenesilicas. *ACS applied materials & interfaces*. **2015**, 7(12), 6792-6802.
147. Dassanayake, R.S.; Gunathilake, C.; Dassanayake, A.C.; Abidi, N.; Jaroniec, M. Amidoxime-functionalized nanocrystalline cellulose-mesoporous silica composites for carbon dioxide sorption at ambient and elevated temperatures. *J. Mater. Chem. A*. **2017**, 5(16), 7462-7473.
148. Gunathilake, C.; Dassanayake, R.S.; Abidi, N.; Jaroniec, M. Amidoxime-functionalized microcrystalline cellulose-mesoporous silica composites for carbon dioxide sorption at elevated temperatures. *J. Mater. Chem. A*. **2016**, 4(13), 4808-4819.
149. Gunathilake, C.; Jaroniec, M. Mesoporous calcium oxide-silica and magnesium oxide-silica composites for CO<sub>2</sub> capture at ambient and elevated temperatures. *J. Mater. Chem. A*. **2016**, 4(28), 10914-10924.
150. Gunathilake, C., Dassanayake, R.S., Kalpage, C.S. and Jaroniec, M. Development of Alumina-Mesoporous Organosilica Hybrid Materials for Carbon Dioxide Adsorption at 25° C. *Materials*. **2018**, 11(11), 2301.
151. Gunathilake, C.; Gangoda, M.; Jaroniec, M. 2013. Mesoporous isocyanurate-containing organosilica-alumina composites and their thermal treatment in nitrogen for carbon dioxide sorption at elevated temperatures. *J. Mater. Chem. A*. **2013**, 1(28), 8244-8252.
152. Gunathilake, C.; Jaroniec, M. Mesoporous alumina-zirconia-organosilica composites for CO<sub>2</sub> capture at ambient and elevated temperatures. *J. Mater. Chem. A*. **2015**, 3(6), 2707-2716.

153. Choi, W.; Min, K.; Kim, C. Ko, Y.S.; Jeon, J.W.; Seo, H.; Park, Y.K.; Choi, M. Epoxide-functionalization of polyethyleneimine for synthesis of stable carbon dioxide adsorbent in temperature swing adsorption. *Nature communications*. **2016** 7(1), 1-8.
154. Hu, Y.; Liu, W.; Yang, Y.; Qu, M.; Li, H. 2019. CO<sub>2</sub> capture by Li<sub>4</sub>SiO<sub>4</sub> sorbents and their applications: current developments and new trends. *J. Chem. Eng.* **2019**, 359, 604-625.
155. Wang, L.; Yang, R.T. Increasing selective CO<sub>2</sub> adsorption on amine-grafted SBA-15 by increasing silanol density. *J. Phys. Chem. C* **2011**, 115(43), 21264-21272.
156. Rafigh, S.M.; Heydarinasab, A., 2017. Mesoporous chitosan-SiO<sub>2</sub> nanoparticles: synthesis, characterization, and CO<sub>2</sub> adsorption capacity. *ACS Sustain. Chem. Eng.* **2017**, 5(11), 10379-10386.
157. Yang, J.; Li, J.; Wang, W.; Li, L.; Li, J. Adsorption of CO<sub>2</sub>, CH<sub>4</sub>, and N<sub>2</sub> on 8-, 10-, and 12-membered ring hydrophobic microporous high-silica zeolites: DDR, silicalite-1, and beta. *Ind. Eng. Chem. Res.* **2013**, 52(50), 17856-17864.
158. Zohdi, S.; Anbia, M.; Salehi, S. Improved CO<sub>2</sub> adsorption capacity and CO<sub>2</sub>/CH<sub>4</sub> and CO<sub>2</sub>/N<sub>2</sub> selectivity in novel hollow silica particles by modification with multi-walled carbon nanotubes containing amine groups. *Polyhedron*. **2019**, 166, 175-185.
159. Fernandes, J.; Fernandes, A.C.; Echeverría, J.C.; Moriones, P.; Garrido, J.J.; Pires, J. Adsorption of gases and vapours in silica based xerogels. *Colloids and Surfaces A: Physicochemical and Engineering Aspects*. **2019**, 561, 128-135.
160. Liu, X.; Gao, F.; Xu, J.; Zhou, L.; Liu, H.; Hu, J. Zeolite@ Mesoporous silica-supported-amine hybrids for the capture of CO<sub>2</sub> in the presence of water. *Microporous and Mesoporous Materials*. **2016**, 222, 113-119
161. Wei, L.; Jing, Y.; Gao, Z.; Wang, Y. 2015. Development of a pentaethylenhexamine-modified solid support adsorbent for CO<sub>2</sub> capture from model flue gas. *Chinese Journal of Chemical Engineering*. **2015**, 23(2), 366-371.
162. Yan, X.; Zhang, L.; Zhang, Y.; Yang, G.; Yan, Z. Amine-modified SBA-15: effect of pore structure on the performance for CO<sub>2</sub> capture. *Industrial & Engineering Chemistry Research*. **2011**, 50(6), 3220-3226.
163. Zhang, X.; Qin, H.; Zheng, X.; Wu, W. Development of efficient amine-modified mesoporous silica SBA-15 for CO<sub>2</sub> capture. *Materials Research Bulletin*. **2013**, 48(10), 3981-3986.
164. Chen, C.; Son, W.J.; You, K.S.; Ahn, J.W.; Ahn, W.S. Carbon dioxide capture using amine-impregnated HMS having textural mesoporosity. *Chemical Engineering Journal*. **2010**, 161(1-2), 46-52.
165. Subagyo, D.J.; Marshall, M.; Knowles, G.P.; Chaffee, A.L. CO<sub>2</sub> adsorption by amine modified siliceous mesostructured cellular foam (MCF) in humidified gas. *Microporous and mesoporous materials*. **2014**, 186, 84-93.
166. Ma, J.; Liu, Q.; Chen, D.; Wen, S.; Wang, T. CO<sub>2</sub> adsorption on amine-modified mesoporous silicas. *J. Porous Mater.* **2014**, 21(5), 859-867.
167. Zhang, H.; Goeppert, A.; Prakash, G.S.; Olah, G. Applicability of linear polyethylenimine supported on nano-silica for the adsorption of CO<sub>2</sub> from various sources including dry air. *RSC Advances*. **2015**, 5(65), 52550-52562.
168. Wang, X.; Chen, L.; Guo, Q. Development of hybrid amine-functionalized MCM-41 sorbents for CO<sub>2</sub> capture. *Chemical Engineering Journal*. **2015**, 260, 573-581.
169. Liu, J.L.; Lin, R.B. Structural properties and reactivities of amino-modified silica fume solid sorbents for low-temperature CO<sub>2</sub> capture. *Powder technology*. **2013**, 241, 188-195.
170. Li, K.; Jiang, J.; Tian, S.; Yan, F.; Chen, X. Polyethyleneimine-nano silica composites: a low-cost and promising adsorbent for CO<sub>2</sub> capture. *J. Mater. Chem. A*. **2015**, 3(5), 2166-2175.
171. Li, K.; Jiang, J.; Yan, F.; Tian, S.; Chen, X. The influence of polyethyleneimine type and molecular weight on the CO<sub>2</sub> capture performance of PEI-nano silica adsorbents. *Applied energy*. **2014**, 136, 750-755.
172. Quang, D.V.; Hatton, T.A.; Abu-Zahra, M.R. Thermally stable amine-grafted adsorbent prepared by impregnating 3-aminopropyltriethoxysilane on mesoporous silica for CO<sub>2</sub> capture. *Ind. Eng. Chem. Res.* **2016**, 55(29), 7842-7852.
173. Zeng, W.; Bai, H. High-performance CO<sub>2</sub> capture on amine-functionalized hierarchically porous silica nanoparticles prepared by a simple template-free method. *Adsorption*. **2016**, 22(2), 117-127.
174. Linneen, N.N.; Pfeffer, R.; Lin, Y.S. CO<sub>2</sub> adsorption performance for amine grafted particulate silica aerogels. *Chemical Engineering Journal*. **2014**, 254, 190-197.
175. Le, Y.; Guo, D.; Cheng, B.; Yu, J. Amine-functionalized monodispersed porous silica microspheres with enhanced CO<sub>2</sub> adsorption performance and good cyclic stability. *J. Colloid Interface Sci.* **2013**, 408, 173-180.
176. Singh, B.; Polshettiwar, V. 2016. Design of CO<sub>2</sub> sorbents using functionalized fibrous nanosilica (KCC-1): insights into the effect of the silica morphology (KCC-1 vs. MCM-41). *J. Mater. Chem. A*. **2016**, 4(18), 7005-7019.
177. Zhang, L.; Zhan, N.; Jin, Q.; Liu, H.; Hu, J. Impregnation of polyethylenimine in mesoporous multilamellar silica vesicles for CO<sub>2</sub> capture: a kinetic study. *Ind. Eng. Chem. Res.* **2016**, 55(20), 5885-5891.



178. Zhou, L.; Fan, J.; Cui, G.; Shang, X.; Tang, Q.; Wang, J.; Fan, M. Highly efficient and reversible CO<sub>2</sub> adsorption by amine-grafted platelet SBA-15 with expanded pore diameters and short mesochannels. *Green Chemistry*. **2014**, 16(8),4009-4016.
179. Mittal, N.; Samanta, A.; Sarkar, P.; Gupta, R. Postcombustion CO<sub>2</sub> capture using N-(3-trimethoxysilylpropyl) diethylenetriamine-grafted solid adsorbent. *Energy Sci. Eng.***2015**, 3(3), 207-220.
180. Yao, M.; Dong, Y.; Feng, X.; Hu, X.; Jia, A.; Xie, G.; Hu, G.; Lu, J.; Luo, M.; Fan, M. The effect of post-processing conditions on aminosilane functionalization of mesocellular silica foam for post-combustion CO<sub>2</sub> capture. *Fuel*. **2014**,123, 66-72.
181. Ko, Y.G.; Lee, H.J.; Kim, J.Y.; Choi, U.S.; 2014. Hierarchically porous aminosilica monolith as a CO<sub>2</sub> adsorbent. *ACS Appl. Mater. Interfaces*.**2014**, 6(15), 12988-12996.
182. Shi, X.; Xiao, H.; Azarabadi, H.; Song, J.; Wu, X.; Chen, X.; Lackner, K.S. Sorbents for the direct capture of CO<sub>2</sub> from ambient air. *Angewandte Chemie International Edition*. **2020**. 59(18), 6984-7006.

**Disclaimer/Publisher's Note:** The statements, opinions and data contained in all publications are solely those of the individual author(s) and contributor(s) and not of MDPI and/or the editor(s). MDPI and/or the editor(s) disclaim responsibility for any injury to people or property resulting from any ideas, methods, instructions or products referred to in the content.